Tampere University

Joonas Lång

# FEASIBILITY AND ENERGY EFFICIENCY OF FREQUENCY CONVERTER DRIVEN SYNCHRONOUS RELUCTANCE MACHINE IN CRANE APPLICATION

Master of Science Thesis
Faculty of Information Technology and Communication Sciences
Examiner: Associate Professor Petros Karamanakos
September 2023

# ABSTRACT

Joonas Lång: Feasibility and Energy Efficiency of Frequency Converter Driven Synchronous Reluctance Machine in Crane Application
Master of Science Thesis
Tampere University
Master's Degree Programme in Electrical Engineering
September 2023

---

Cranes can use frequency converter driven electrical machines to realize variable speed operations. This thesis discusses if industry favourite induction machine could be replaced by synchronous reluctance machine. Comparative tests have proposed that synchronous reluctance machine is more energy efficient than induction machine. Feasibility of this electrical machine for crane applications needs to be reviewed if this replacement is to be considered. Feasibility and energy efficiency is examined by presenting the operational principles of the compared electrical machines and conducting practical tests with synchronous reluctance machine against a load machine.
Presented theory and comparative tests presented no objections against synchronous reluctance machine used for crane application. Practical tests display that synchronous reluctance machine can produce enough torque for crane applications. Tested motor handled zero-speed test cases remarkably well. The motor followed speed commands satisfactorily. Efficiency test results were too low with the tested motor. Efficiency tests faced difficulties, due to which the results are not accurate, but the results can be used to give an indicative view of the efficiency of the tested machine. Synchronous reluctance machine could be used instead of induction machine in cranes, but feasibility requires further research.

Keywords: Synchronous reluctance machine, Crane, Frequency converter, Induction machine

# TIIVISTELMÄ

Joonas Lång: Taajuusmuuttajaohjatun reluktanssitahtikoneen soveltuvuus ja energiatehokkuus nosturikäytössä
Diplomityö
Tampereen yliopisto
Sähkötekniikan diplomi-insinöörin tutkinto-ohjelma
Syyskuu 2023

---

Nosturit voivat hyödyntää taajuusmuuttajaohjattuja sähkökoneita tuottaakseen sähkömoottorikäytön, jota voidaan ohjata monilla eri nopeuksilla. Tämä diplomityö selvittää voitaisiinko teollisuuden suosima oikosulkukone korvata reluktanssitahtikoneella. Vertailevat kokeet ovat osoittaneet, että reluktassitahtikoneella on parempi hyötysuhde kuin oikosulkukoneella. Jotta tämä korvaus voitaisiin tehdä, reluktanssitahtikoneen soveltuvuus nosturikäytöön tulee selvittää. Soveltuvuutta ja energiatehokkuutta tutkitaan esittämällä vertailtavien sähkökoneiden toimintaperiaatteet ja suorittamalla käytännön kokeita reluktanssitahtikoneella kuormakonetta vastaan.
Esitetty teoria ja vertailevat kokeet eivät osoittaneet esteitä reluktanssitahtikoneen käytölle nostureissa. Käytännönkokeet osoittivat, että reluktanssitahtikone kykenee tuottamaan tarpeeksi vääntömomenttia nosturikäyttöön. Testimoottori hallitsi kiitettävästi testit, joissa moottorinnopeus pidettiin nollassa kuormaa vastaan. Moottori seurasi nopeuskomentoja tyydyttävästi. Hyötysuhdetestien tulokset olivat liian matalat testimoottorilla. Hyötysuhdetestien aikana kohdattiin ongelmia, joiden seurauksena tulokset eivät ole tarkkoja, mutta tuloksia voidaan käyttää suuntaa antavina. Reluktanssitahtikonetta voidaan käyttää oikosulkukoneen sijasta nostureissa, mutta soveltuvuus vaatii lisää tutkimusta.

Avainsanat: Reluktanssitahtikone, Nosturi, Taajuusmuuttaja, Oikosulkukone

# PREFACE

This thesis was written for the Inverter Development team at Konecranes. Associate Professor Petros Karamanakos supervised my work from the university and M.Sc. Tommi Paksunen acted as my supervisor from the company.

I would like to thank both of my supervisors Petros Karamanakos and Tommi Paksunen for their help with writing the thesis. Special thanks to M.Sc. Mikko Porma for lending his expertise regarding crane applications and my manager Marko Venäläinen for offering this interesting thesis work. I would also like to thank M.Sc. Matias Matilainen and Iiro Paananen for their aid with building the test setup used for practical tests.

Hyvinkää, 28.09.2023

Joonas Lång

# CONTENTS

# LIST OF FIGURES

# LIST OF SYMBOLS AND ABBREVIATIONS

| | |
|---|---|
| AC | Alternating current |
| DC | Direct current |
| DOL | Direct online |
| DTC | Direct torque control |
| FOC | Field-oriented control |
| IEC | International Electrotechnical Commission |
| IM | Induction machine |
| MTPA | Maximum torque per ampere |
| PI | Proportional-integral |
| PLC | Programmable logic controller |
| PWM | Pulse-width modulation |
| RFOC | Rotor field-oriented control |
| RPM | Revolutions per minute |
| RTG | Rubber tyred gantry |
| SFOC | Stator field-oriented control |
| SVM | Space vector modulator |
| SynRM | Synchronous reluctance machine |
| TLSynRM | Transversally laminated synchronous reluctance machine |
| VSI | Voltage source inverter |

| | |
|---|---|
| $a$ | transmission ratio |
| $b$ | turns ratio |
| $c$ | transformation angle modifier |
| $D$ | friction coefficient |
| $\boldsymbol{E}$ | electric field vector |
| $e_s$ | induced voltage in the stator |
| $e_r$ | induced voltage in the rotor |
| $e_{ro}$ | induced voltage in the rotor with locked rotor |
| $e'_r$ | induced voltage in the rotor referred to the stator |
| $\boldsymbol{F}$ | force vector |
| $\boldsymbol{F}_{mag}$ | magnetic force vector |
| $\boldsymbol{F}_{\mu}$ | friction force vector |
| $f_s$ | stator frequency |
| $f_{sw}$ | switching frequency |
| $f_r$ | rotor frequency |
| $f_1$ | desired output frequency |
| $\boldsymbol{G}$ | gravitational force vector |
| $\boldsymbol{g}$ | gravitational acceleration vector |
| $i_d$ | current d-axis value |
| $i_D$ | damper winding current in d-axis |
| $i_{dsc}$ | d-axis current command |
| $i_q$ | current q-axis value |
| $i_Q$ | damper winding current in q-axis |
| $i_{qsc}$ | q-axis current command |
| $i_m$ | magnetizing current |
| $i_r$ | rotor current |
| $i'_r$ | rotor current referred to the stator |
| $i_{rd}$ | rotor current in d-axis |
| $i_{rq}$ | rotor current in q-axis |
| $i_s$ | stator current |
| $i_{s,max}$ | maximum stator current |
| $i_{sd}$ | stator current in d-axis |

| | |
|---|---|
| $i_{sq}$ | stator current in q-axis |
| $i_{sq,limit1}$ | current limit for stator current in q-axis in region 1 |
| $i_{sq,limit2}$ | current limit for stator current in q-axis in region 2 |
| $i_{sU}$ | stator three-phase current U |
| $i_{sV}$ | stator three-phase current V |
| $i_{sW}$ | stator three-phase current W |
| $i_{s\alpha}$ | stator current in α-axis |
| $i_{s\beta}$ | stator current in β-axis |
| $i_{s0}$ | stator current zero-sequence component |
| $J$ | current density |
| $l$ | length of a conductor |
| $L_d$ | d-axis inductance |
| $L_m$ | magnetizing inductance |
| $L_{md}$ | magnetizing inductance in d-axis |
| $L_{mq}$ | magnetizing inductance in q-axis |
| $L_q$ | q-axis inductance |
| $L_r$ | rotor winding self-inductance |
| $L_{r\sigma}$ | rotor leakage inductance |
| $L_s$ | stator inductance |
| $L_{s\sigma}$ | stator leakage inductance |
| $m$ | mass |
| $m_a$ | amplitude modulation ratio |
| $m_f$ | frequency modulation ratio |
| $n_r$ | rotational speed of the rotor in RPM |
| $n_s$ | synchronous speed in RPM |
| $P$ | power |
| $P_{cu}$ | copper losses |
| $P_{drive}$ | input power of the motor drive |
| $P_{in}$ | input power |
| $P_{jrot}$ | rotor losses |
| $P_{jstat}$ | stator losses |
| $P_{loss}$ | total losses |
| $P_{mech}$ | mechanical power |
| $P_{motor}$ | input power of the motor |
| $P_{out}$ | output power |
| $r$ | radius of a round object |
| $R$ | resistance of a conductor |
| $R_c$ | iron losses resistance |
| $R_r$ | rotor resistance |
| $R'_r$ | rotor resistance referred to stator |
| $R_s$ | stator resistance |
| $S$ | surface area |
| $S_U$ | switch command for phase U |
| $S_V$ | switch command for phase V |
| $S_W$ | switch command for phase W |
| $s$ | slip |
| $T$ | torque |
| $T_d$ | drum torque |
| $T_e$ | electrical torque |
| $T_{e,IM}$ | electrical torque of an induction machine |
| $T_l$ | load torque |
| $t$ | time |
| $u_{dc}$ | DC-link voltage |
| $u_{rd}$ | rotor voltage in d-axis |
| $u_{rq}$ | rotor voltage in q-axis |

| | |
|---|---|
| $u_s$ | stator voltage |
| $u_{s,max}$ | maximum stator voltage |
| $u_{sd}$ | stator voltage in d-axis |
| $u_{sq}$ | stator voltage in q-axis |
| $u_{UN}$ | phase voltage U in respect to zero |
| $u_{Uref}$ | phase voltage U reference value |
| $u_{Vref}$ | phase voltage V reference value |
| $u_{Wref}$ | phase voltage W reference value |
| $u_{VN}$ | phase voltage V in respect to zero |
| $u_{UV}$ | line-to-line voltage between the phase U and V |
| $\hat{u}_{control}$ | peak amplitude of control signal |
| $u_{tri}$ | triangular control signal |
| $\hat{u}_{tri}$ | peak amplitude of triangular control signal |
| $\boldsymbol{v}$ | velocity |
| $X_m$ | magnetizing reactance |
| $X_r$ | rotor leakage reactance |
| $X'_r$ | rotor leakage reactance referred to the stator |
| $X_s$ | stator leakage reactance |
| | |
| $\delta_s$ | load angle |
| $\varepsilon$ | induced voltage |
| $\eta_{drive}$ | efficiency of the motor drive |
| $\eta_{motor}$ | efficiency of the motor |
| $\theta_r$ | rotor angle |
| $\kappa$ | current angle |
| $\mu$ | friction coefficient |
| $\rho$ | resistivity of the conductor |
| $\sigma$ | leakage coefficient |
| $\tau$ | rotor time constant |
| $\phi$ | magnetic flux |
| $\varphi$ | phase angle |
| $\Psi_m$ | air gap flux linkage |
| $\Psi_r$ | rotor magnetic flux linkage |
| $\Psi_{rc}$ | command value for rotor flux linkage |
| $\Psi_{rd}$ | rotor magnetic flux linkage in d-axis |
| $\Psi_{rq}$ | rotor magnetic flux linkage in q-axis |
| $\Psi_s$ | stator magnetic flux linkage |
| $\Psi_{sd}$ | stator magnetic flux linkage in d-axis |
| $\Psi_{sq}$ | stator magnetic flux linkage in q-axis |
| $\Psi_{s\sigma}$ | stator leakage flux linkage |
| $\omega$ | angular speed |
| $\omega_d$ | drum angular speed |
| $\omega_e$ | electrical angular speed |
| $\omega_g$ | rotational speed of the reference frame |
| $\omega_m$ | motor angular speed |
| $\omega_r$ | rotational speed of the rotor |
| $\omega_{ref}$ | speed reference |
| $\omega_{sl}$ | angular speed of the slip |

# 1. INTRODUCTION

There has been a growing interest in increasing the energy efficiency of operations in different industries. One method in order to increase the energy efficiency has been to compare different electrical machines, that have been designed using different operational principles, and try to find whether they could be more energy efficient than the industry favorite induction machine. The synchronous reluctance machine is one of these candidates. These electrical machines were already built and tested at the beginning of the 20$^{th}$ century, but they were too inefficient[1]. Modern synchronous reluctance machines have their rotor redesigned for more efficient operations, which offers higher torque per current ratios and better power factors. When using frequency converters, the rotor of the synchronous reluctance machine does not require a cage winding, which increases the efficiency of the electrical machine. These improvements produce a combination that challenges the favored position of induction machine for applications where variable speed operation is desired.

The aim of this thesis is to assess the feasibility and energy efficiency of synchronous reluctance machine drive for crane application. This is realized by presenting and comparing the operational principles of synchronous reluctance machine and induction machine. The motor control of these electrical machines is also discussed. Practical tests are also conducted on the synchronous reluctance machine to confirm its behavior in practical applications. These tests and the presented theory are used to make conclusions on the usability of the machine for crane applications.

In Chapter 2 different cranes and their working principles are presented. Next in Chapter 3 frequency converter is introduced and pulse-width modulation is discussed. Operational principles of induction machine are reviewed in Chapter 4. Chapter 5 presents

the operational principles of synchronous reluctance machine. In the following Chapter 6 the losses that occur in electrical machines are considered. Induction machine and synchronous reluctance machine are compared with each other and conclusions are made based on the presented theory in Chapter 7. Crane application requirements are also declared in this chapter. Chapter 8 discusses preparations and plans for the practical tests of a synchronous reluctance machine. In Chapter 9 the results of practical tests are shown and analyzed. Finally, Chapter 10 presents the conclusions of this thesis.

# 2. CRANE

Crane is a mechanical machine used to lift, lower, and move loads, where the load is connected with the machinery by a rope, chain, or a similar type of construct. There are no other sources of force that help with moving the load other than the force that is being applied through the rope.[2] Generally, when a heavier object needs to be lifted, a crane is required. Cranes can usually be found at factories or construction sites, where heavy construction material, for example, concrete blocks or steel girders, needs to be hoisted. Docks are also an important use environment for cranes, where loading and unloading of cargo of a ship requires mechanical assistance. Container crates are heavy, and their weight can be expressed in tons, which requires greater hoisting forces. For these purposes, bigger cranes might be required, that can be specialized in loading and unloading operations of the cargo of a ship. Similarly, hoisting cases, where the lifted objects are lighter, a smaller crane would be preferable to save in expenses, and to still complete the required work.

## 2.1 Crane types

Depending on the hoisting case, there are many types of cranes, that can be utilized for the most efficient operation. Cranes can be assembled to fit stationary workplaces, for example factories. Mobile versions of cranes can be also constructed if the operation requires movement from the crane. Next, some basic crane types are introduced and elaborated further.

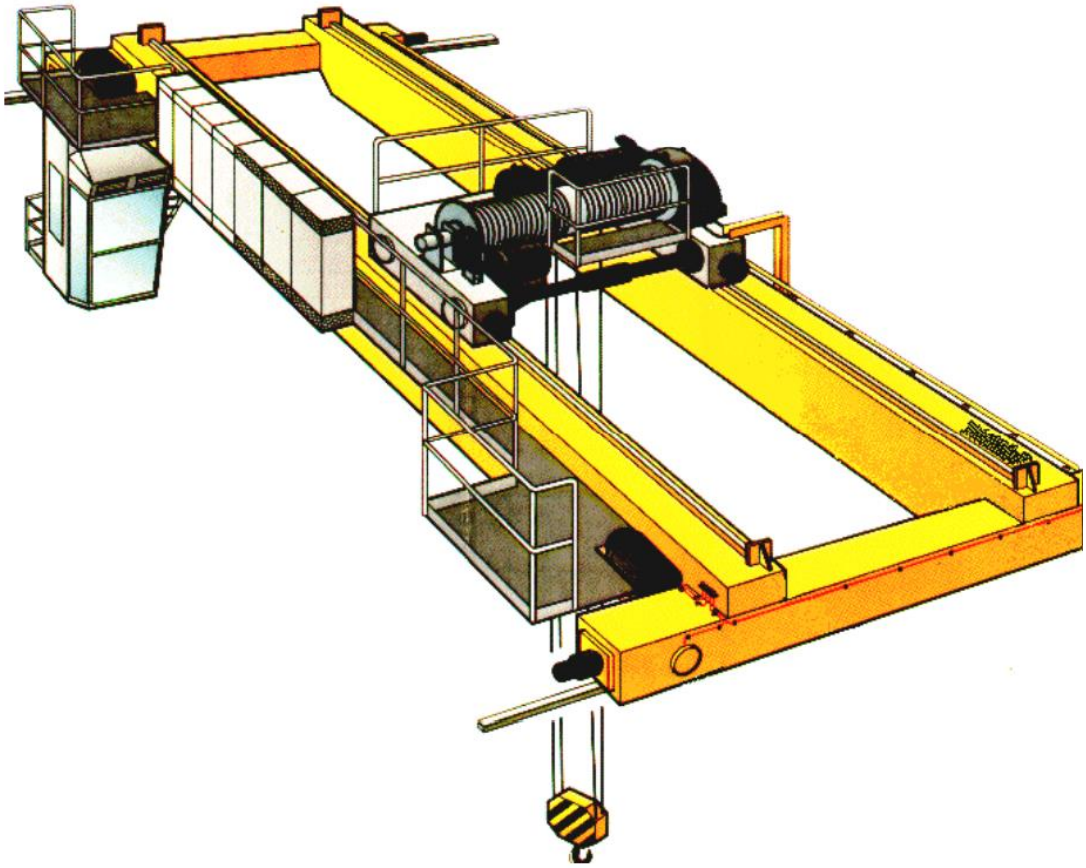

***Figure 1.*** *Bridge crane with two main girders [2].*

Bridge cranes have a main girder, referred to as a bridge, that carries all the machinery needed for hoisting and moving the crane. In this bridge, a trolley is mounted, that can move horizontally along the bridge, and it contains the actual hoisting equipment. It is possible to assemble the crane so, that the bridge can also move horizontally in an orthogonal direction to the earlier mentioned trolley, by adding motors to the bridge and rails for it to move along. Using both of these movements, it is possible to move loads in three dimensions around a certain area. All load movements happen below the crane. Bridge cranes are also called overhead cranes, since they are usually mounted near the ceiling of a building. Bridge can have more than one girder if the crane's structure needs fortifying for heavier hoisting.[2] Figure 1 shows a bridge crane with two main girders, where the trolley is mounted on top of and in between of the girders.


***Figure 2.*** *Rubber tired gantry crane [2].*

Gantry cranes are structurally similar to bridge cranes, with the main girder, referred to as the gantry. This girder has a trolley attached to it, which can move horizontally along the gantry. Gantry is stationary and two posts are supporting it from the ground. It is possible to model the gantry crane to be movable, for example, by creating rails for it in the ground[2]. Other possibility is to attach rubber tires at the bottom of the two supporting posts, making it capable of moving more freely than the rail solution. These cranes are called rubber tired gantry (RTG) cranes[2]. This type of crane is depicted in Figure 2.

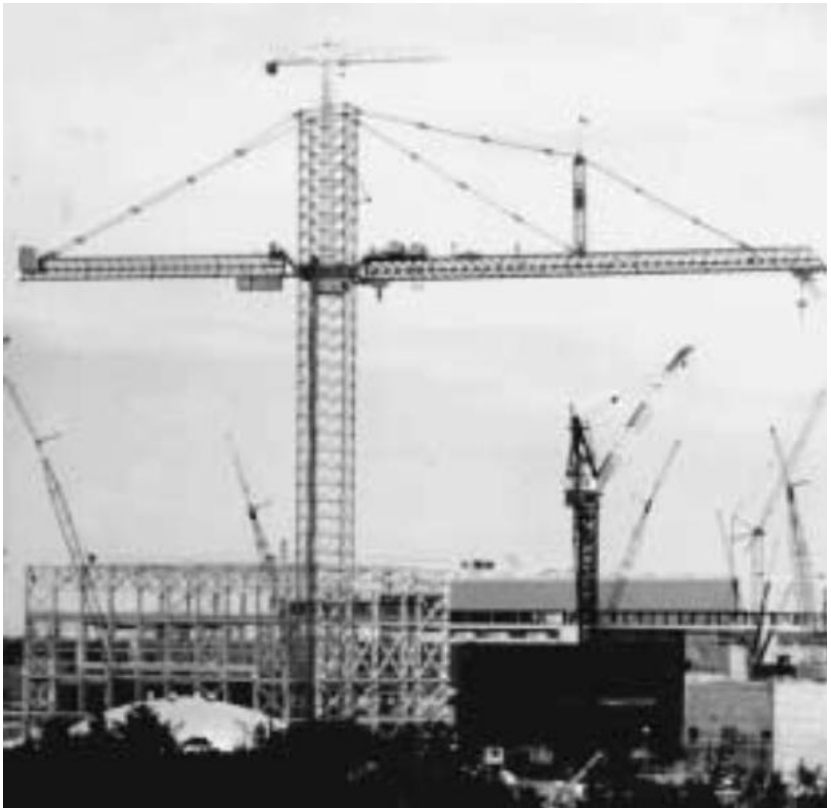

***Figure 3.*** *Rotary crane [3].*

If the main girder only needs to be rotated horizontally, a rotary crane can be chosen for hoisting. These cranes are also called tower cranes. Rotary cranes are tall stationary cranes, that can rotate the girder horizontally to a new position. This allows the trolley moving along the main girder to be operated in a circular area around the crane. These cranes can commonly be seen used in the construction of buildings[3]. Figure 3 shows an example of a rotary crane.


***Figure 4.****Articulated boom crane [2].*

Boom cranes are more compact than the crane types mentioned earlier. If a crane needs to be mounted on a movable object, for example on a ship, boom cranes are the usual solution[3]. Rigid boom crane has a single weight -carrying girder, which is called jib, that has been articulated to handle loads. One variant of the boom crane, called the articulated boom crane, has another jib behind the first jib. This structure allows the crane to move loads almost only in a horizontal direction[2]. An example of an articulated boom crane can be seen in Figure 4.

## 2.2 Hoisting and horizontal movement

In the following two sections, the movement of the load in horizontal and vertical direction is considered for bridge- and gantry cranes. Load movement relies on similar principles for these crane types, due to their comparable structure. Cases where load is moved horizontally or vertically should be considered separately, due to differing force and control mechanics.

### 2.2.1 Hoisting

Load hoisting requires more energy than moving it horizontally. Machinery needs to output enough force to counteract the pull of the gravity on the load. In Figure 5, the basic structure for hoisting is presented.

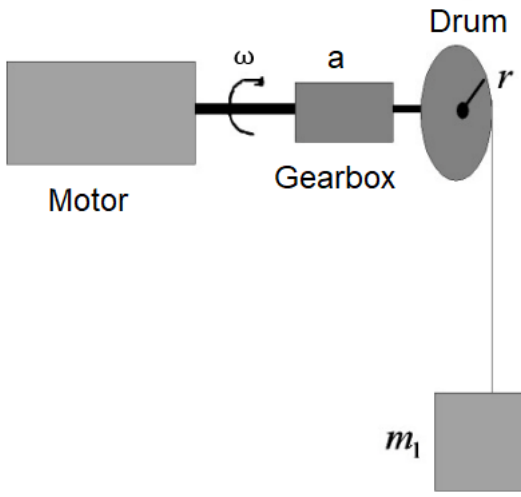


***Figure 5.*** *Basic structure for hoisting, modified from [4].*

The crane can receive the required hoisting force from, for example, a combustion engine or an electrical motor. This force is called torque. Torque is conducted through a gearbox, which allows changing of rotational speed and magnitude of torque, to better fit the desired hoisting case. Next the rotational force is transformed into linear force, by using it to rotate a drum, that has the hoisting rope reeled around it. Thus, the torque

produced by the motor either reels the rope in or releases it, moving the load in a vertical direction. The direction of load's movement depends on the rotational direction of the drum. Separate brake is used to prevent the rotation of the drum when no movement is required. This brake needs to be opened if the load needs to be moved, and closed after the operation is done, so the load stays still.

Power required to hoist an object can be expressed by [1]

$$P = T\omega \tag{1}$$

where $P$ is required power, $T$ is torque, and $\omega$ is angular speed. Since a gearbox is used, torque and angular speed are different for the motor and the drum used to hoist the load. Assuming lossless operation from gearbox, the relation between motor and drum can be expressed by [1]

$$\frac{T_\mathrm{l}}{T_\mathrm{d}} = \frac{\omega_\mathrm{d}}{\omega_\mathrm{m}} = \mathrm{a} \tag{2}$$

where $T_\mathrm{l}$ is motor torque applied to the axle, $T_\mathrm{d}$ is drum torque, $\omega_\mathrm{d}$ is angular speed of the drum, $\omega_\mathrm{m}$ is angular speed of the motor shaft, and $a$ is transmission ratio. The motor also needs to produce more torque to counteract the effects of friction and inertia. Earlier equation used only load torque, but the full equation that displays the torque mechanics of the motor can be expressed by [1]

$$T_\mathrm{e} = T_\mathrm{l} + J\frac{d\omega}{dt} + D\omega \tag{3}$$

where $T_\mathrm{e}$ is electrical torque, $T_\mathrm{l}$ is load torque, $J$ is inertia, $d\omega/dt$ is angular acceleration, and $D$ is friction coefficient. Electrical torque is all the torque the motor produces, while load torque is actually what is used to hoist the load. The relation between rotational force and linear force can be expressed by

$$\boldsymbol{T} = \boldsymbol{F}r \tag{4}$$

where $\boldsymbol{F}$ is the linear force vector and $r$ is the radius of the rotating object. With Equation (4), the torque required to hoist the load can be defined. Load is pulled down by gravitational force, and an equal amount of force needs to be exerted, if the load needs to move at a steady speed. According to Equation (3), if acceleration is needed, a greater force, or in this case torque, is required to counteract the effects of inertia. Gravitational force vector can be defined as

$$\boldsymbol{G} = m\boldsymbol{g} \tag{5}$$

where $m$ is the mass of the lifted object and $\boldsymbol{g}$ is the gravitational acceleration vector, usually defined as 9,81 m/s$^2$.

### 2.2.2 Horizontal movement

With horizontal movement, the trolley carrying the hoisting equipment, is moved along the gantry or bridge of the crane. Bridge cranes can also move the main girder horizontally. Horizontal movement requires less energy when compared with hoisting, since the work does not need to offset all the gravitational force. In this type of movement, gravity affects the work through friction by pulling the load and the crane downwards. Force required to move the object depends on its weight. Also, the force of friction is different depending on whether the object is moved from a standstill or it is already moving. For these two cases, practical tests have been conducted to define friction coefficients. The materials of two chafing objects also affect the force of friction and different friction coefficients have been defined for these cases. Friction equation can be presented as

$$\boldsymbol{F}_{\mu} = \mu m\boldsymbol{g} \tag{6}$$

where $\boldsymbol{F}_{\mu}$ is force vector caused by friction, $\mu$ is the friction coefficient and $m$ is mass. In this case mass refers to the whole moving object and not just the lifted load. The trolley

with its lifting equipment adds to the moving weight. For bridge cranes in the case of moving the main girder, the main girder's weight needs to be considered as well.

The crane can be equipped with dedicated motors for horizontal movement which are attached to the trolley or, in the case of a bridge crane, to the main girder. Motors are fixed to both sides of the movable object, and it is important to make sure these motors move the object at the same speed.

# 3. FREQUENCY CONVERTER

Advances in power electronics have created methods in order to control power in more accurate and energy-efficient ways. Frequency converters are capable of producing voltage of variable frequency and magnitude, which can be used to operate the electrical machine in variable speeds. This allows the motor to take only the required amount of power from the grid and allows the user to drive the motor with more accuracy and in an expanded range of operation. In this section frequency converters are considered mainly for motor drive applications.

## 3.1 Frequency converter with an intermediate DC link

The frequency converter consists of many power electronics components that are used to convert the input voltage into desired output voltage that can have varying frequency and magnitude. Input voltage is AC voltage that is taken from the grid. This voltage needs to be transformed into DC voltage first by using a power electronics converter called the rectifier. Rectified voltage is then lead into a section that is called the DC-link, which has a capacitor that is used to smooth out the converted voltage and store energy. From there the next section is the inverter. The inverter is a converter that is used to transform DC voltage into AC voltage, and this produced AC voltage is the output of the frequency converter. Inverters designed for this configuration are also called voltage source inverters (VSI).[5], [6] The structure of this operation can be seen in Figure 6.

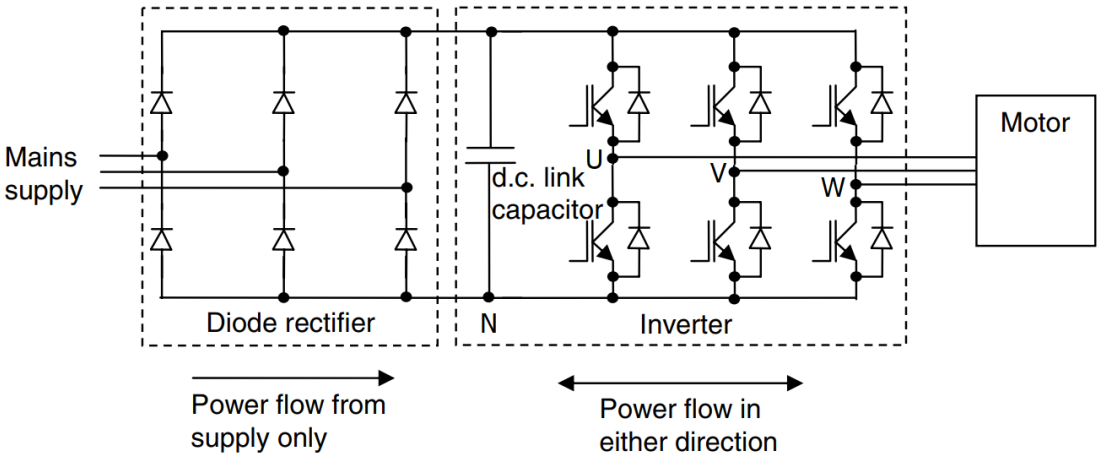


***Figure 6.*** *Example structure of an intermediate DC link frequency converter, modified from [6].*

Figure 6 shows one possible way to implement this desired operation. It is possible to produce a rectifier or an inverter using different power electronic devices to better fit the requirements of the operation. In this case, the rectifier is created with diodes, which only allow the power to flow in one direction, which would be in this case from the input AC side to the DC side. If the operation doesn't require the frequency converter to input power back into the grid, this method is cheap and easy to implement. If this is however desired, the rectifier can be built as an active rectifier. This circuit is presented in Figure 7. The inverter is created using controllable semiconductor switches. This allows the frequency converter to output voltage at desired magnitudes and frequencies, which allows the motor to be driven at different speeds.[5], [6]

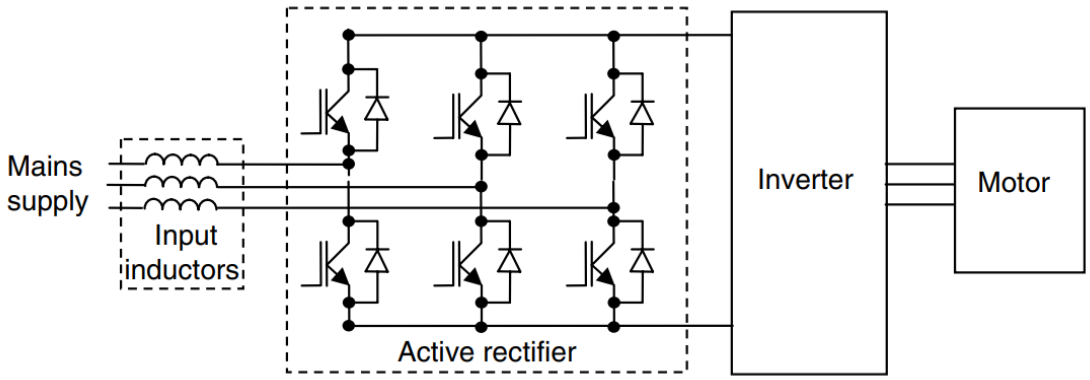


***Figure 7.*** *Frequency converter using an active rectifier [6].*

When braking an electric motor, power is generated and this power is conducted into the frequency converter. The output inverter now acts as a rectifier and leads the converted power into the DC link. This generated power needs to be handled and there are several ways to do this. One easy method is to use a braking resistor that dissipates the generated power into heat. Figure 8 shows a configuration using a braking resistor. DC link voltage magnitude is monitored, and when it crosses the maximum defined value, the braking resistor is connected into the circuit. Resistors resistance needs to be chosen carefully so the resistor is capable of handling all the generated power.[6]

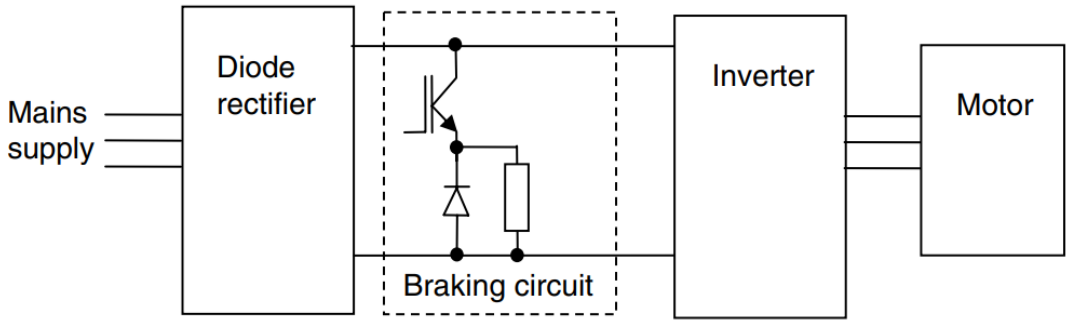


***Figure 8.*** *Frequency converter with a braking resistor [6].*

The braking resistor is not an energy efficient method so another method might be required. If the rectifier is built as an active rectifier, it is possible to input the generated energy back into the grid. Another benefit is that the active rectifier can produce better quality currents than the diode rectifier. However, this method is more expensive and requires its own control circuit.[6]

If neither of these methods is desired, braking can be controlled so the DC link voltage is maintained within acceptable range. The produced extra power is dissipated in losses that occur in the frequency converter and motor. One way to handle the extra power is to use it to increase the magnetizing current of the motor, and in this way dissipate it in the stator losses. This however means, that the rate of deceleration might be lowered to handle the generated power. In cases with more powerful motors or high-speed operations, this method can be considered unusable, if the deceleration needs to occur relatively quickly.[5], [6]

## 3.2 Pulse width modulation (PWM)

Frequency converter uses power electronics converters to convert DC voltage into AC and vice versa using semiconductor switches. These switches need to be controlled for these operations, by opening and closing them in certain patterns. Pulse width modulation is one modulation method that can be used to implement this operation.

With this method the output voltage of a frequency converter can be produced in the form of a square wave or resembling a sinusoidal wave. For this section, the sinusoidal output will be discussed since it is the more popular option. This output is not perfectly sinusoidal and contains many discontinuity points, but the fundamental-frequency component of the line voltage resembles a sinusoidal wave. In this method, a triangular control signal $u_{tri}$ is used that fluctuates at a frequency which is called switching frequency. The triangular control signal is compared with a sinusoidal control signal and with this a variable frequency voltage and magnitude can be produced. For a three phased output, three separate sinusoidal control signals need to be used. These signals are 120 degrees out of phase of each other. Figure 9 shows an example of this control.[5]

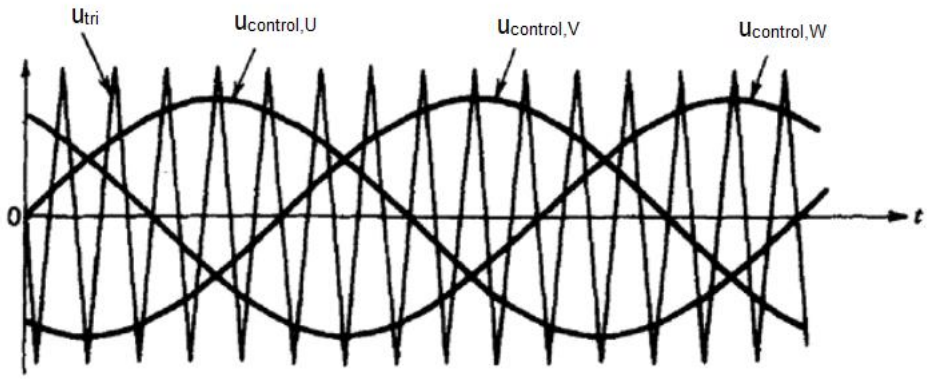


***Figure 9.*** *Three phase sinusoidal pulse width modulation, modified from [5].*

For a three phased output the inverter has three legs, which each consist of 2 semiconductor switches, and each of these legs control one phase. This can be seen in Figure 6. Sinusoidal pulse-width modulation controls the opening and closing of these switches by comparing the phases reference signal to the triangular control signal. If the sinusoidal phase control signal has a higher value than the triangular control signal, the switch conducts. In a reverse situation, the switch is opened. Figure 10 displays output voltages $u_{UN}$ and $u_{VN}$, that have been produced following the control signals of Figure 9. This figure also shows how the produced line-to-line voltage $u_{UV}$ would look like and how it resembles the fundamental voltage $u_{LL1}$.[5]

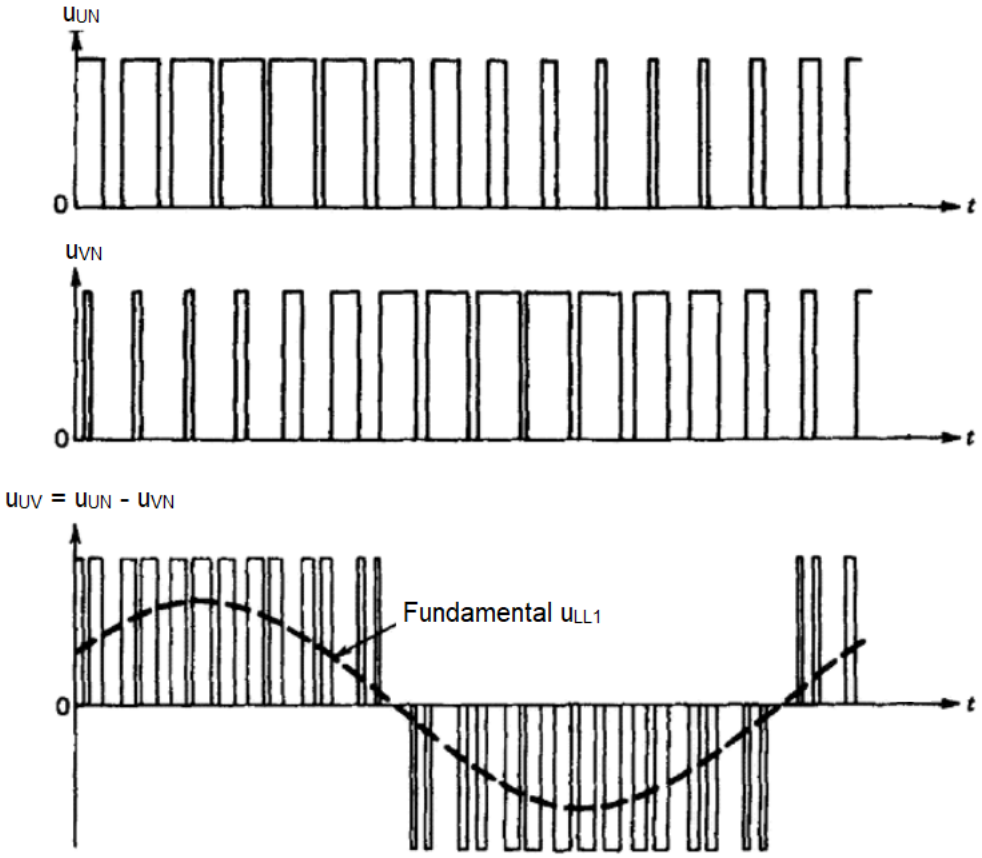


***Figure 10.*** *Line-to-line voltage $u_{UV}$ produced with PWM, modified from [5].*

Space vector modulation (SVM) is another modulation method that is used. Dissimilar to sinusoidal pulse width modulation, where the per phase amplitudes of the control signals determine the operation of the switches, space vector modulation creates the switching sequences according to the reference space vector, which is received from the control circuit. There are 8 different switch combinations, which creates 7 unique space vectors, which are used to create the desired output.[7] Figure 11 displays these space vectors. Space vectors are explained in relation to the motor control in Chapter 4.3.1.

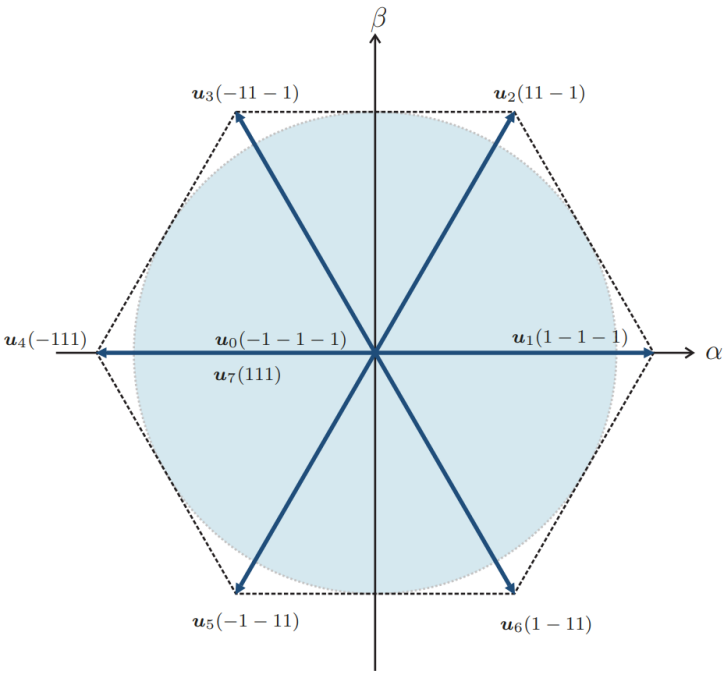


***Figure 11.*** *Space vectors used in SVM [8].*

To help with modulation, two modulation ratios can be defined as

$$m_{\mathrm{a}} = \frac{\hat{u}_{\mathrm{control}}}{\hat{u}_{\mathrm{tri}}} \tag{7}$$

where $m_{\mathrm{a}}$ is the amplitude modulation ratio, $\hat{u}_{\mathrm{control}}$ is the amplitude of the reference signal and $\hat{u}_{\mathrm{tri}}$ is the amplitude of the triangular control signal. Frequency modulation ratio can be defined as

$$m_{\mathrm{f}} = \frac{f_{\mathrm{sw}}}{f_1} \tag{8}$$

where $f_{\mathrm{sw}}$ is switching frequency and $f_1$ is the fundamental frequency of the output voltage.[5]

Switching frequency is usually chosen as high as possible to produce the best output, because as the switching frequency is increased, the switches are operated more often which produces an output that more closely resembles a sinusoidal wave. However, there is a drawback to this. Semiconductor losses increase as the switches are operated more often. Higher switching frequencies can also be beneficial, since the acous-

tic noise that human ear can hear can be reduced, which can improve the user experience. Choosing the most fitting switching frequency needs to carefully considered for different applications, balancing the earlier mentioned gain and disadvantage.[5]

Amplitude modulation ratio $m_a$ is usual kept in between 0 and 1, so when using a sinusoidal PWM, the output voltage would vary linearly with $m_a$. However, this will limit the maximum voltage of the frequency converter since the amplitude modulation ratio defines the amplitude of the output. It is possible to increase the $m_a$ over 1 to produces a higher maximum voltage and this method is called overmodulation. This, however, will create more harmonics in the output.[5] There is a method called Min-Max injection, where a zero sequence signal, which consists of odd triple harmonics, is added in to the reference voltage signal, which makes it possible for the linear modulation to continue over the modulation ratio of 1. With this method, the final limit for linear modulation for amplitude modulation ratio is $2 / \sqrt{3}$, which is approximately 1,1547.[7]

# 4. INDUCTION MACHINE

Induction machines are the workhorse of the industry and they can be found in many motor applications. Their technology is well understood and can be considered technologically mature with their simple and rugged structure. The main aspect of this thesis is to evaluate the properties of the synchronous reluctance machine, but it is also important to present the working principles of the induction machine, since induction machines are the industry favorite. By doing this, these two electric machines can be better compared with each other, and from this a comparative analysis can be produced, which will be presented in a later section of this thesis. Electrical machine is a term used to comprehensively describe these machines, but the term electrical motor is usually used, since these machines are used in motor applications. However, electrical machines are inherently capable of acting as a generator as well. Switching between motor and generator operation is possible while the machine is being driven.

## 4.1 Structure

Like electrical machines usually, an induction machine consists of a stator and a rotor, that are cylindrically shaped. The stator is hollowed out from the inside and the rotor is assembled inside. There is a small air gap in between the stator and the rotor. The stator is used to produce a rotating magnetic field in the air gap and this causes the rotor to turn. The rotating rotor is then used to move the mechanical load the machine is connected to. Figure 12 displays the basic structure of an induction machine.

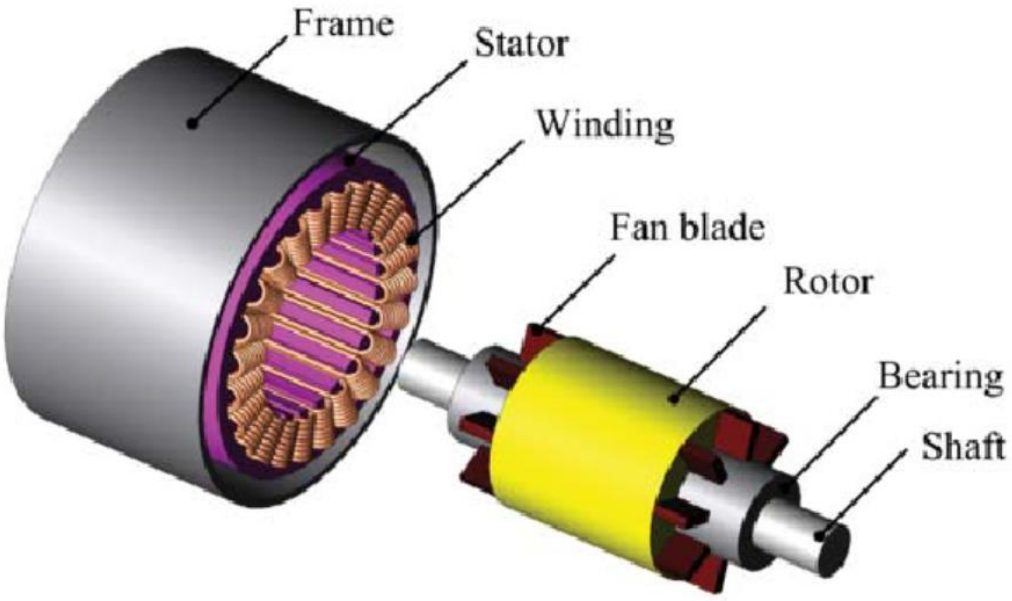


***Figure 12.*** *Induction machine structure [9].*

### 4.1.1 Stator

The input current of an induction machine is conducted into the stator of this machine, which creates a magnetic field. To produce a rotating magnetic field in the air gap, the stator can be built with distributed windings. This can be seen in Figure 13, where the stator has 6 winding slots. These stator slots are evenly distributed around it, which in a three-phase motor form two poles per phase. When the input of the induction motor is three-phase alternating current, this current is conducted through the windings around the stator slots, and this produces a rotating magnetic field in the air gap.[9]

With the slot configuration presented in Figure 13, the rotating magnetic field in the air gap wouldn't be perfectly sinusoidal, due to space harmonics that are caused by the non-sinusoidal placement of the slots. The produced output can be smoothed by adding more slots to the rotor, increasing the amount of slots that is allocated to each phase. This will, however, increase the production cost of the motor.[10]

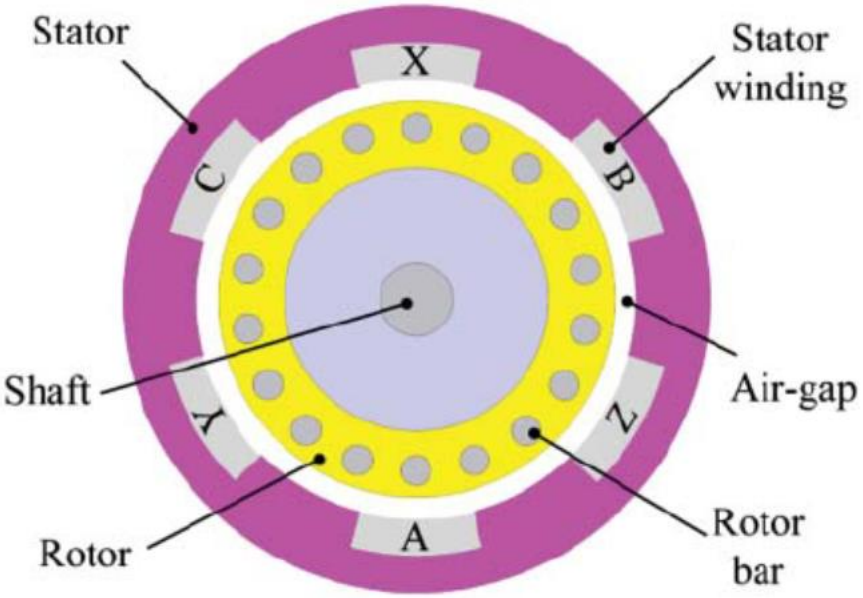


***Figure 13.*** *Cross section view of induction machine [9].*

### 4.1.2 Rotor

The rotor of an induction machine has a cylindrical core, that is made of laminated electrical steel, and winding conductors around the core. These winding conductors can be built in two ways, with slip rings or a squirrel cage. In a slip ring machine, the windings are constructed in similarly with the stator and the number of pole pairs needs to be also the same. In this winding configuration, the rotor winding is connected to a circuit outside of the machine with slip rings and brushes. This allows the rotor resistance to be changed during use, but the structure requires more maintenance due to the brushes and more losses are caused. Induction machines using this rotor type are less popular than the squirrel cage construct and are mostly used in special applications, for example in wind turbines. The squirrel cage rotor will be mainly considered in this thesis, as it is the most used rotor solution for induction machines. [1]

Squirrel cage induction machines are the popular option, where the rotor core has conductor rails die-cast into the slots in the surrounding core. It is also possible to replace

the conductor rails with precast copper rods that are soldered or welded into the laminated steel core. In both of these methods, the rods are short-circuited with short-circuit end rings. Figure 14 depicts the cage structure of this rotor type.[1]

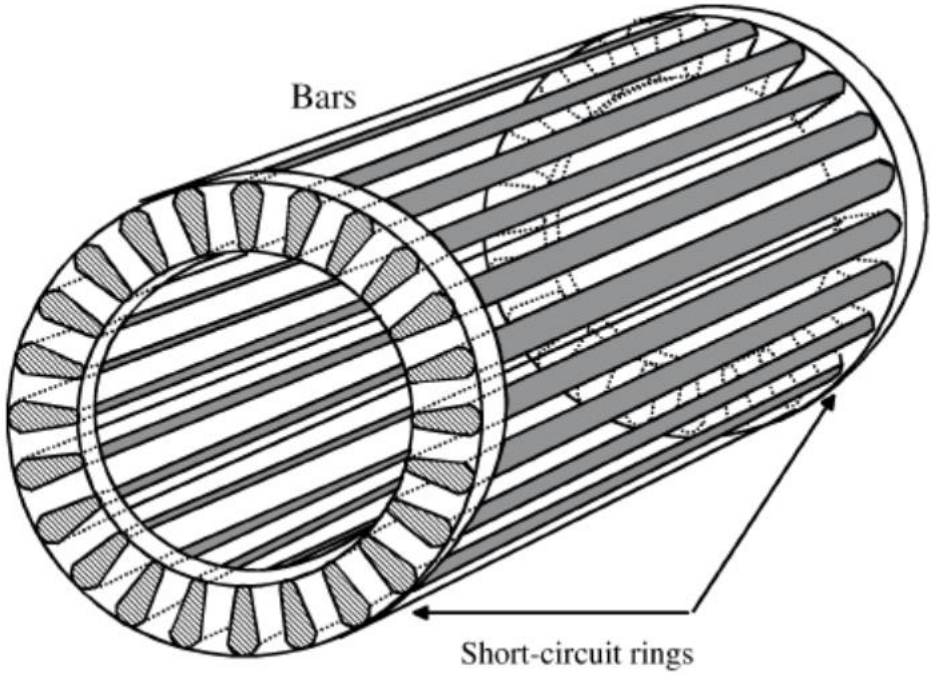


***Figure 14.*** *Squirrel cage of an induction machine [11].*

Materials used to build the rotor cage depend on the use case of the motor and the power classification. Aluminum is the cost-effective material for motors rated below 37 kW and copper bars are used for over 50 kW applications, since rotor losses are smaller with copper than aluminum. Aluminum is also preferable material in lower operations compared with cast iron, since it resists corrosion better, is easier to work with, has lesser weight and better heat conduction attributes. In applications with the power classification of over 37 kW cast iron can be used instead of aluminum, to strengthen the mechanical structure of the rotor for high torque operations.[6]

## 4.2 Operational Principles

Induction machines are asynchronous machines. This means that the rotational speed of the rotor and the magnetic field in the air gap differs. Stator creates a rotating mag-

netic field and the speed it rotates at is referred to as synchronous speed. In motor applications the rotor rotates at a slightly lower speed than the synchronous speed. This speed difference is called slip angular speed. The slip is mandatory for the induction motor to produce torque and the principles of this feature will be presented in this section along with other details pertaining to the operational principles.

Slip can be calculated by

$$s = \frac{n_\mathrm{s} - n_\mathrm{r}}{n_\mathrm{s}} \tag{9}$$

where $n_\mathrm{s}$ is the synchronous speed and $n_\mathrm{r}$ is the rotational speed of the rotor. In this equation, the slip is presented in per-unit form. In motor applications, the slip receives values in between of 0 and 1. Synchronous speed can be solved in revolutions per minute (RPM) by

$$n_s = \frac{60 f_s}{p} \tag{10}$$

where $f_\mathrm{s}$ is the stator frequency and $p$ is the pole pair number of the used induction machine. Combining Equations (9) and (10) the rotor's rotational speed can be presented as

$$n_\mathrm{r} = \frac{60 f_\mathrm{s}}{p}(1 - s) \tag{11}$$

where $n_\mathrm{r}$ is in RPM.[1]

For an induction machine to produce torque, a rotating time changing magnetic field is required in the air gap between the stator and the rotor. According to Faraday's law, this rotating magnetic field induces voltage into the rotor rods that are short circuited. Faraday's law can be expressed with equation

$$\varepsilon = -\frac{d\phi}{dt} \tag{12}$$

where $\varepsilon$ is the induced voltage and $\phi$ is the magnetic flux flowing through the open surface. It can be seen from the Equation (12) that the induced voltage has a negative value, and this occurs because the flux generated by induced currents opposes the magnetic field that induced these currents.[10]

Induced currents create a magnetic field around them and this generates force. This can be expressed with Lorentz force law, which can be written as

$$\boldsymbol{F}_{\mathrm{mag}} = q[\boldsymbol{E} + (\boldsymbol{v} \times \boldsymbol{B})] \tag{13}$$

where $q$ is the charge, $\boldsymbol{E}$ is the electric field vector, $\boldsymbol{v}$ is the velocity vector the charge moves at and $\boldsymbol{B}$ is the magnetic flux density vector. Due to this force generated by the magnetic field, that is produced by the induced currents, the rotor rotates and induction machine generates torque.[10]

To better explain the working principles of an induction machine, an equivalent circuit can be built, which resembles how a transformer operates. Figure 14 displays the single-phase equivalent circuit.

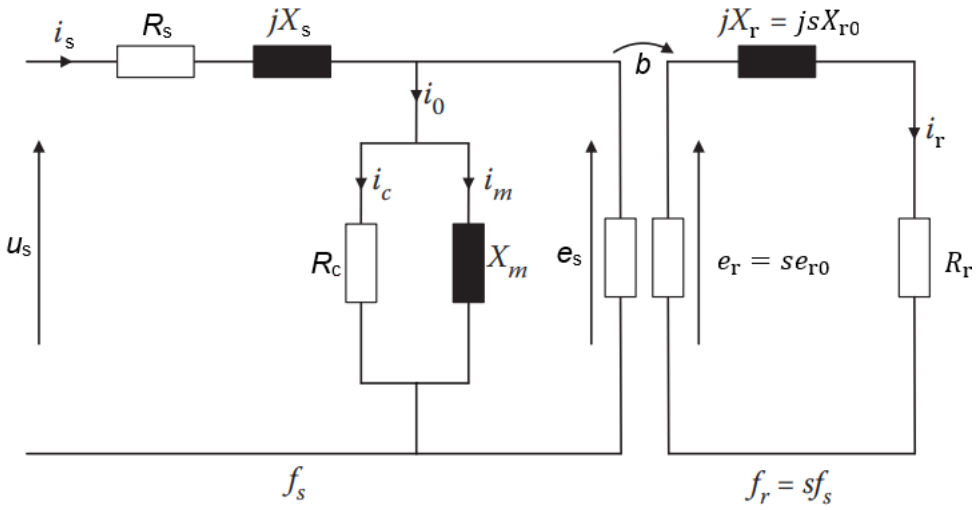


***Figure 15.*** *Single phase equivalent circuit of an induction machine, modified from [10].*

In Figure 15 $e_s$ is the induced voltage in the stator, $u_s$ the stator voltage, $i_s$ the stator current, $R_s$ the stator resistance, $X_s$ the stator leakage reactance and $b$ the turns ratio. Symbols on the right are respective values for the rotor. Stator side of the equivalent

circuit also has a branch with variables for magnetization and iron losses. These values are: $i_m$ the magnetizing current, $X_m$ the magnetizing reactance and $R_c$ which is used to represent iron losses. The voltage induced to the rotor depends on slip and this can be expressed with

$$e_r = se_{r0} \tag{14}$$

where $e_{r0}$ is the induced voltage when rotor is locked in place, meaning that the slip is 1.[10]

With the current equation, the total impedance on the rotor side can be written as

$$i_r = \frac{se_{r0}}{R_r + jsX_{r0}} = \frac{e_{r0}}{\frac{R_r}{s} + jX_{r0}} \tag{15}$$

$$Z_r = \frac{R_r}{s} + jX_{r0} \tag{16}$$

Rotor resistance component in Equation (16) can be divided into

$$\frac{R_r}{s} = R_r + R_r\left(\frac{1-s}{s}\right) \tag{17}$$

where the first term presents the rotor copper losses and the second term presents the electromechanical power conversion.[10]

The equivalent circuit can be simplified by referring the rotor values to the stator side by converting the rotor values with following equations:

$$e_r' = b^2 e_{r0} \tag{18}$$

$$R_r' = b^2 R_r \tag{19}$$

$$i_r' = \frac{i_r}{b} \tag{20}$$

$$X_r' = b^2 X_r \tag{21}$$

These values can be used to redraw the equivalent circuit in Figure 15. The revised equivalent circuit is presented in Figure 16.

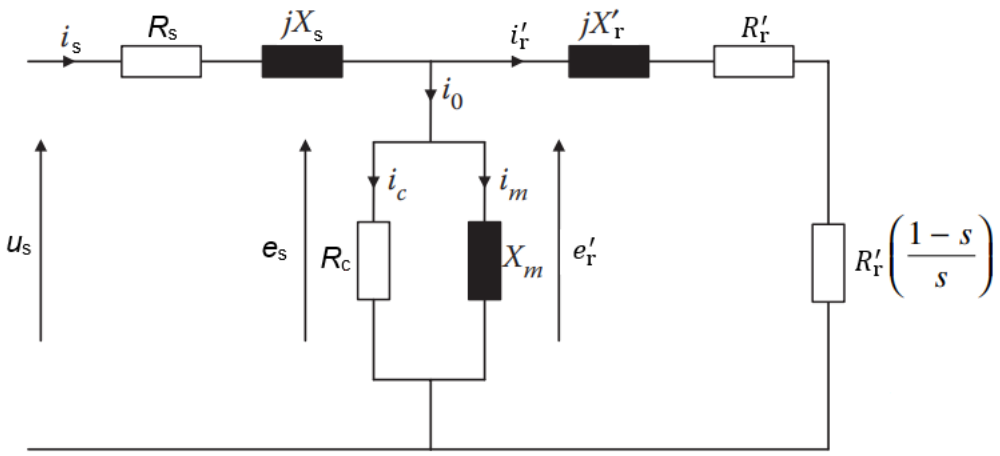


***Figure 16.*** *Equivalent circuit of an induction machine referred to the stator, modified from [10].*

## 4.3 Motor Control

The induction machine can be driven by connecting it directly to the grid. This will, however, limit the speed of the machine to operate only at the grid's frequency. If a variable speed operation is required, a frequency converter can be used to control the speed of the machine. This also allows a smoother operation of the machine. There are many control strategies for controlling an induction machine desirably, but before these methods are introduced, a space vector presentation of the machine is examined first. After this the scalar control and field-oriented control are presented.

### 4.3.1 Space vector presentation

Space vectors are used to represent a three-phased quantity with a single vector in a complex plane. A two-axis presentation is usually chosen and this transformation can be done for stator current as an example by

$$\begin{bmatrix} i_{s\alpha} \\ i_{s\beta} \\ i_{s0} \end{bmatrix} = \frac{2}{3} \begin{bmatrix} \cos c & \cos(c+120°) & \cos(c+240°) \\ \sin c & \sin(c+120°) & \sin(c+240°) \\ \frac{1}{2} & \frac{1}{2} & \frac{1}{2} \end{bmatrix} \begin{bmatrix} i_{sU} \\ i_{sV} \\ i_{sW} \end{bmatrix} \tag{22}$$

where $i_{sU}$, $i_{sV}$ and $i_{sW}$ are three-phase values of the stator current. The term $c$ is usually chosen to be 0 and the 2/3 term is added to make the transformation amplitude invariant. In symmetric cases for a three-phase system, the zero-sequence component $i_{s0}$ is

nonexistent and can be ignored. This transformation can be performed for any three-phase variable, in which case the current vector on the right-hand side of the Equation 22 is changed to the desired variable.[1]

Equation (22) produces two variables that have a phase difference of 90°. The control of the electrical machine can be further simplified by removing the rotation from these two variables by aligning them to a rotating frame of reference. This is performed with

$$i_{\mathrm{sd}} = i_{\mathrm{s}\alpha} \cos \omega_{\mathrm{g}} t + i_{\mathrm{s}\beta} \sin \omega_{\mathrm{g}} t \tag{23}$$

$$i_{\mathrm{sq}} = -i_{\mathrm{s}\alpha} \sin \omega_{\mathrm{g}} t + i_{\mathrm{s}\beta} \cos \omega_{\mathrm{g}} t \tag{24}$$

where $\omega_{\mathrm{g}}$ is the rotation speed of the reference frame. This produces stable values that allow the AC machine to be controlled like a DC machine if the inspected variable rotates at the same speed as the reference frame.[1] Figure 17 presents the earlier produced space vector values.

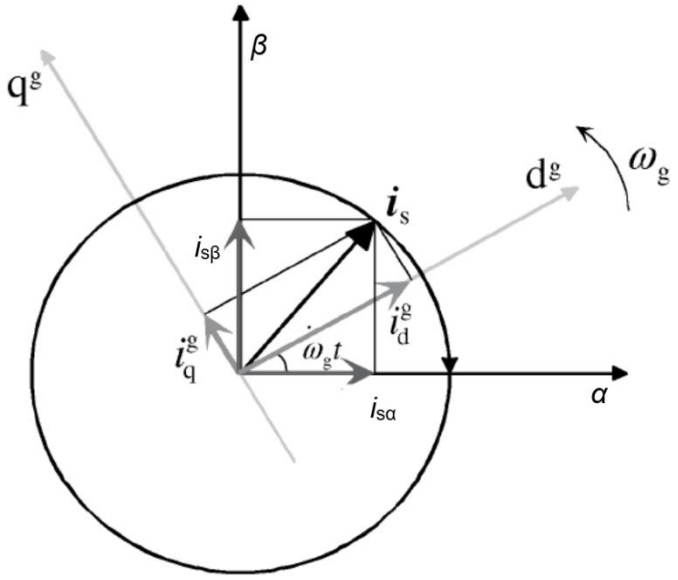


***Figure 17.*** *Stator current space vector values in different reference frames, modified from [1].*

The rotating reference frame can be used to transform the equivalent circuit of the induction machine into a rotating model as well. This equivalent circuit is presented in Figure 18.

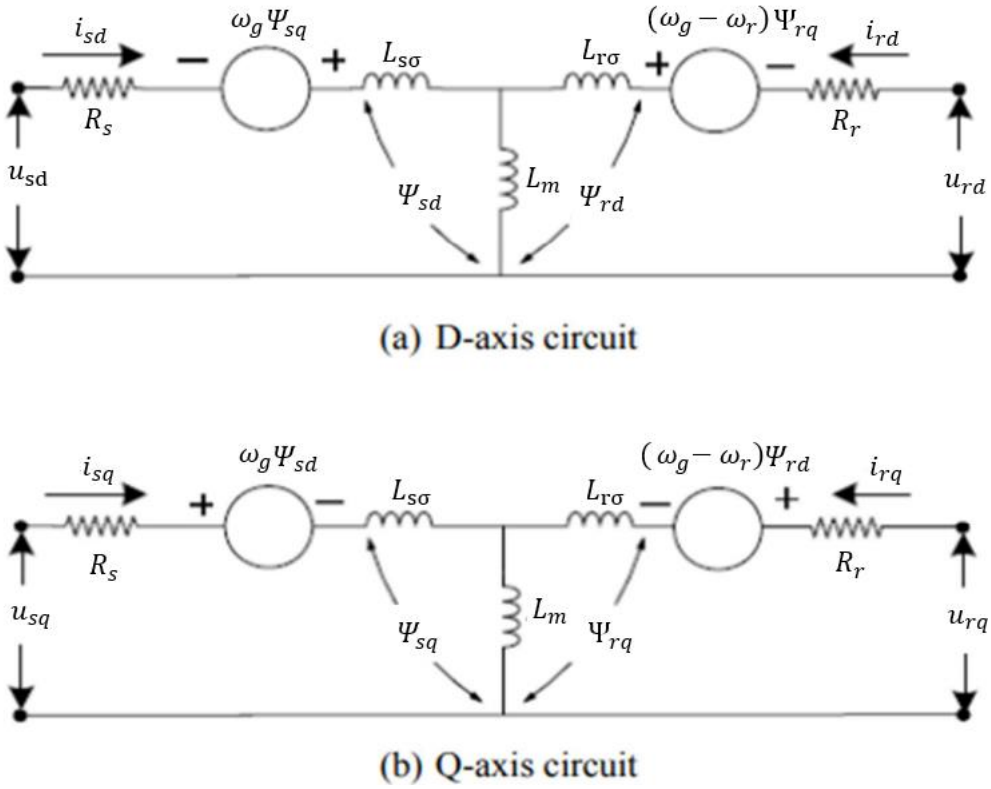


***Figure 18.*** *Equivalent circuit of an induction machine in d- and q-axis presentation. Modified from [12].*

Values in Figure 18 can be written in equation form as

$$u_{\mathrm{sd}} = R_s i_{sd} + \frac{d\Psi_{sd}}{dt} - \omega_g \Psi_{sq} \tag{25}$$

$$u_{sq} = R_s i_{sq} + \frac{d\Psi_{sq}}{dt} + \omega_g \Psi_{sd} \tag{26}$$

$$u_{rd} = 0 = R_r i_{rd} + \frac{d\Psi_{rd}}{dt} - (\omega_g - \omega_r)\Psi_{rq} \tag{27}$$

$$u_{rq} = 0 = R_r i_{rq} + \frac{d\Psi_{rq}}{dt} + (\omega_g - \omega_r)\Psi_{rd} \tag{28}$$

where $\Psi_{sd}$ and $\Psi_{sq}$ are stator flux linkages in dq reference frame, $\omega_g$ rotation speed of the reference frame and $\omega_r$ is the rotational speed of the rotor. Subscripts d and q are used to refer a parameter to either axis. Flux linkage terms can be defined by

$$\Psi_{\mathrm{sd}} = (L_{s\sigma} + L_{\mathrm{m}})i_{\mathrm{sd}} + L_{\mathrm{m}} i_{\mathrm{rd}} \tag{29}$$

$$\Psi_{\mathrm{sq}} = (L_{s\sigma} + L_{\mathrm{m}})i_{\mathrm{sq}} + L_{\mathrm{m}} i_{\mathrm{rq}} \tag{30}$$

$$\Psi_{\mathrm{rd}} = (L_{\mathrm{r}\sigma} + L_{\mathrm{m}})i_{\mathrm{rd}} + L_{\mathrm{m}}i_{\mathrm{sd}} \tag{31}$$

$$\Psi_{\mathrm{rq}} = (L_{\mathrm{r}\sigma} + L_{\mathrm{m}})i_{\mathrm{rq}} + L_{\mathrm{m}}i_{\mathrm{sq}} \tag{32}$$

where $L_{\mathrm{s}\sigma}$ is the stator leakage inductance, $L_{\mathrm{r}\sigma}$ is the rotor leakage inductance and $L_{\mathrm{m}}$ is the magnetizing inductance. Using this model, the equation for torque can be defined as

$$T_{\mathrm{e}} = p\left(\Psi_{\mathrm{sd}}i_{\mathrm{sq}} - \Psi_{\mathrm{sq}}i_{\mathrm{sd}}\right) = p\frac{L_{\mathrm{m}}}{L_{\mathrm{r}}}\left(\Psi_{\mathrm{rd}}i_{\mathrm{sq}} - \Psi_{\mathrm{rq}}i_{\mathrm{sd}}\right) \tag{33}$$

where $p$ is the number of pole pairs and $L_{\mathrm{r}}$ is the rotor winding self-inductance. $L_{\mathrm{r}}$ can be solved with Equation (34).[7]

$$L_{\mathrm{r}} = L_{\mathrm{r}\sigma} + L_{\mathrm{m}} \tag{34}$$

### 4.3.2 Field-oriented control (FOC)

Field-oriented control relies on using a rotating reference frame, that is aligned to a certain variable, for example rotor flux linkage. This allows the transformation of AC quantities into DC, which makes the use of proportional-integral (PI) controllers possible. FOC aims to simplify AC motor control, by making it more analogous to how a separately excited DC machine is controlled. In the induction machine, the stator current is responsible for producing the flux excitation and torque, which makes these values hard to control separately. In separately excited DC-machine, the flux excitation current has its own separate circuit and torque is produced with the armature current. FOC creates a similar situation for AC-machines, by mathematically separating the stator current into flux excitation current $i_{\mathrm{d}}$ and torque producing current $i_{\mathrm{q}}$. These currents only exist in the motor control software. However, these variables can be transformed into voltage commands for the pulse width modulator that produce an outcome, where flux- and torque production are decoupled into separate components, thus making them separately controllable.[7]

Equation (33) presents how torque is calculated for the induction machine. However, this equation depends on both of the currents $i_d$ and $i_q$, while the basic idea of FOC was to make the torque production only dependent on $i_q$. This problem can be solved, and operation made more similar to a DC machine, by aligning the rotating reference frame to the d-component of either stator or rotor flux linkage, which changes the q-component of the chosen variable into zero. These orientations are called rotor field-oriented control (RFOC) and stator field-oriented control (SFOC). With rotor field-oriented control, the d-axis is aligned with d-component of the rotor flux linkage. This sets the rotor flux linkage q-axis component to zero and simplifies rotor voltage Equations (27) and (28) into

$$u_{\mathrm{rd}} = 0 = R_{\mathrm{r}} i_{\mathrm{rd}} + \frac{d\Psi_{\mathrm{rd}}}{dt} \tag{35}$$

$$u_{\mathrm{rq}} = 0 = R_{\mathrm{r}} i_{\mathrm{rq}} + \left(\omega_{\mathrm{g}} - \omega_{\mathrm{r}}\right)\Psi_{\mathrm{rd}} \tag{36}$$

Rotor currents $i_{rd}$ and $i_{rq}$ can be solved from rotor flux linkage Equations (31) and (32) by

$$\Psi_{\mathrm{rd}} = (L_{\mathrm{r}\sigma} + L_{\mathrm{m}}) i_{\mathrm{rd}} + L_{\mathrm{m}} i_{\mathrm{sd}} \;\Rightarrow i_{\mathrm{rd}} = \frac{(\Psi_{\mathrm{rd}} - L_{\mathrm{m}} i_{\mathrm{sd}})}{L_{\mathrm{r}}} \tag{37}$$

$$\Psi_{\mathrm{rq}} = 0 = (L_{\mathrm{r}\sigma} + L_{\mathrm{m}}) i_{\mathrm{rq}} + L_{\mathrm{m}} i_{\mathrm{sq}} \;\Rightarrow i_{\mathrm{rq}} = -\left(\frac{L_{\mathrm{m}}}{L_{\mathrm{r}}}\right) i_{\mathrm{sq}} \tag{38}$$

These rotor currents are then transferred into Equations (35) and (36) which produces

$$\Psi_{\mathrm{r}} + \tau \frac{d\Psi_{\mathrm{r}}}{dt} = L_{\mathrm{m}} i_{\mathrm{sd}} \tag{39}$$

$$\left(\omega_{\mathrm{g}} - \omega_{\mathrm{r}}\right)\Psi_{\mathrm{r}} \tau = L_{\mathrm{m}} i_{\mathrm{sq}} \tag{40}$$

where $\tau$ is the rotor time constant, that is defined with

$$\tau = \frac{L_{\mathrm{r}}}{R_{\mathrm{r}}} \tag{41}$$

In rotor flux linkage reference frame, the torque equation is expressed as

$$T_{\mathrm{e}} = p\left(\frac{L_{\mathrm{m}}}{L_{\mathrm{r}}}\right)\Psi_{\mathrm{rd}} i_{\mathrm{sq}} \tag{42}$$

Currents $i_{\mathrm{sd}}$ and $i_{\mathrm{sq}}$ can be solved from Equations (39) and (42) with

$$i_{sd} = \frac{\Psi_r + \tau \frac{d\Psi_r}{dt}}{L_m} \tag{43}$$

$$i_{sq} = \frac{T_e}{p\left(\frac{L_m}{L_r}\right)\Psi_{rd}} \tag{44}$$

which produces the final equations to model the operation of the rotor field-oriented control.[7]

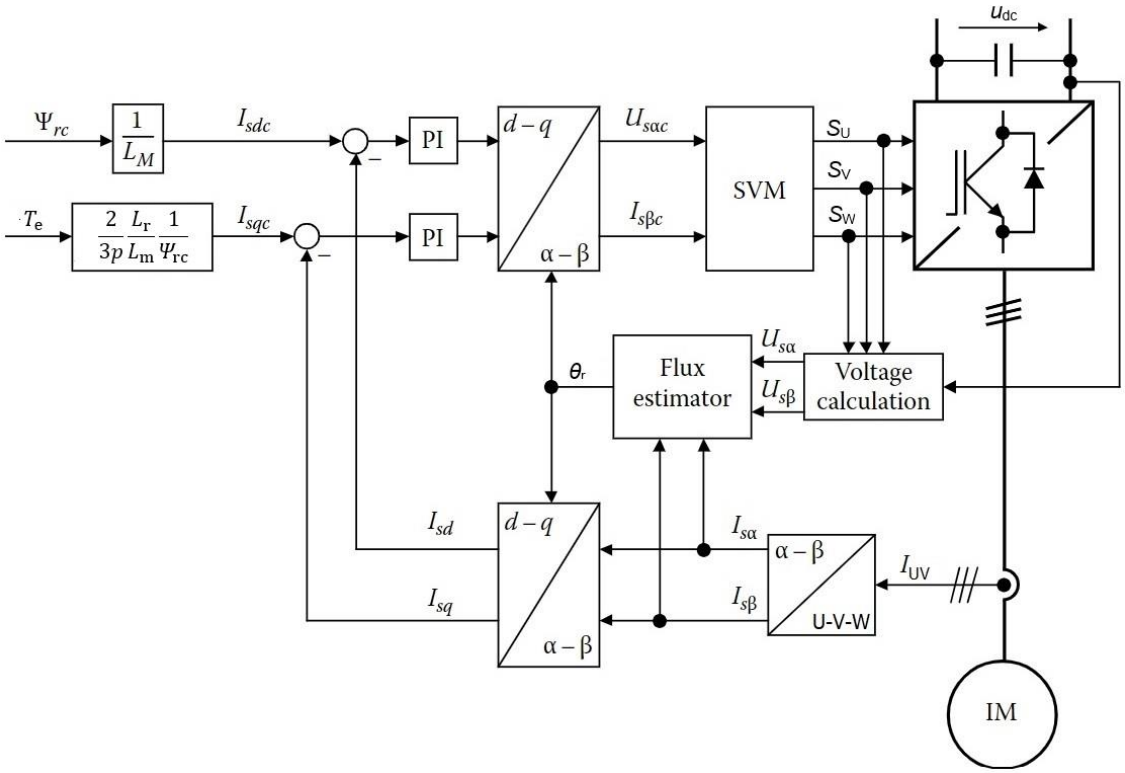


***Figure 19.*** *Direct rotor field-oriented control block diagram for induction machine, modified from [7].*

Field-oriented control can be implemented for the induction machine using a rotor flux reference frame in two ways: with the direct- or indirect method. The main difference with these methods is how the flux vector position is defined, which is used for the ro-

tating coordinate frame transformation. The direct method uses a flux estimator to produce this value. Figure 19 displays a block diagram of this control strategy for the constant flux region. In this figure $S_U$, $S_V$ and $S_W$ are switch commands and $u_{dc}$ is the DC-link voltage. Command values for currents $i_d$ and $i_q$ can be defined from Equations (39) and (42) with a constant flux by

$$i_{\mathrm{sdc}} = \frac{\Psi_{\mathrm{rc}}}{L_{\mathrm{m}}} \tag{45}$$

$$i_{\mathrm{sqc}} = \frac{2}{3p}\frac{L_{\mathrm{r}}}{L_{\mathrm{m}}}\frac{1}{\Psi_{\mathrm{rc}}}T_{\mathrm{e}} \tag{46}$$

where $\Psi_{\mathrm{rc}}$ is the command value for rotor flux linkage.[7]

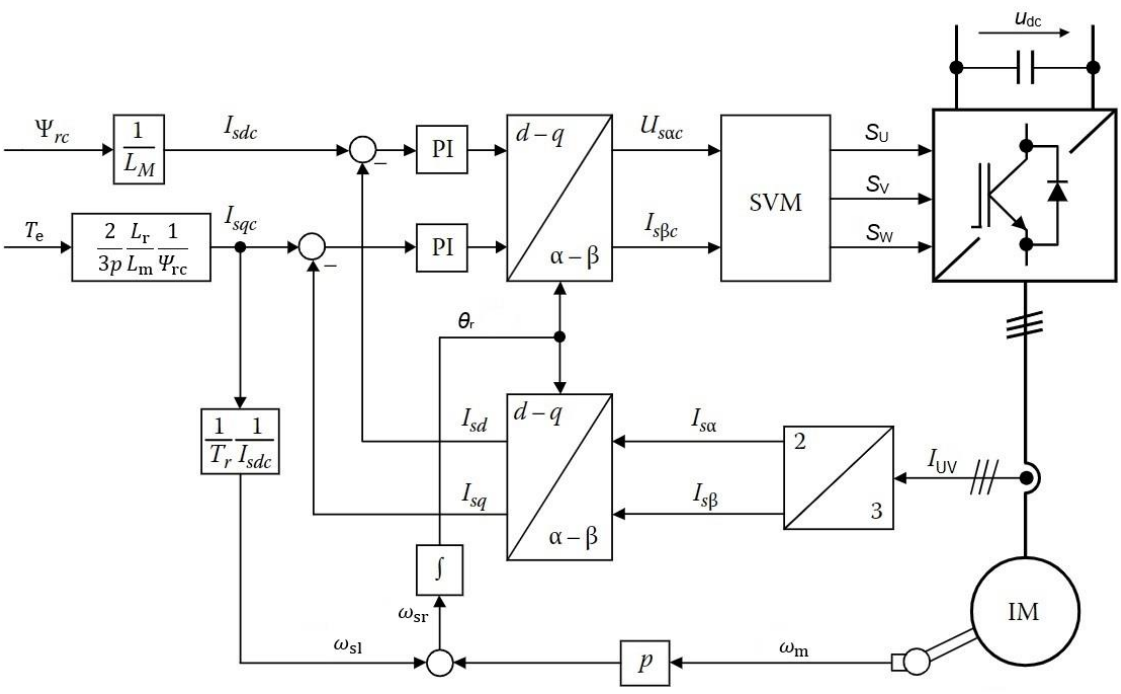


***Figure 20.*** *Indirect rotor field-oriented control block diagram for induction machine, modified from [7].*

Indirect rotor field-oriented control strategy integrates the angular speed of rotor flux vector to produce the rotor flux vector position. This speed is produced by measuring the rotor angular speed and summing it up with slip angular speed, which is presented in equation form with

$$\omega_{\mathrm{sr}} = \omega_{\mathrm{sl}} + p\omega_{\mathrm{m}} \tag{47}$$

where $\omega_{sl}$ is the angular speed of the slip and $\omega_m$ is the mechanical angular speed of the rotor. Angular slip speed can be calculated from Equation (40) with

$$\omega_{\mathrm{sl}} = \frac{1}{i_{\mathrm{sdc}}} \frac{1}{\tau} i_{\mathrm{sqc}} \tag{48}$$

where the subscripts *c* refers the values being command values. Figure 20 presents a block diagram of this control strategy for constant flux region.[7]

# 5. SYNCHRONOUS RELUCTANCE MACHINE

Synchronous reluctance machines (SynRM) have gained more attention in the recent years, as the industry has been investigating methods to improve the energy efficiency of their operations. With improved motor control techniques and research into optimizing the motor design, synchronous reluctance machines are presented as a competitor to the industry favorite induction machine. Many motor application use cases could be replaced with this improved motor[1]. This section presents different methods how a synchronous reluctance machine can be built and outlines the principles how the machine operates. Mathematical models are also built that are used to consider the motor control of this machine.

## 5.1 Structure

The synchronous reluctance machine has a similar structure to induction machine. The stator is built using the same principles of distributed windings that create a rotating sinusoidal magnetic field in the air gap. Design points and notices regarding the stator from Chapter 4.1 are also applicable to this type of electric machine. However, the main difference of these machines comes in the structure of the rotor. While induction machine uses windings or rotor bars in the rotor, the synchronous reluctance machine has neither of these and the rotor usually consists of laminated steel plates. The rotor is shaped and constructed in a way to take advantage of reluctance torque using salient poles, which differs from how the induction machine generates torque.

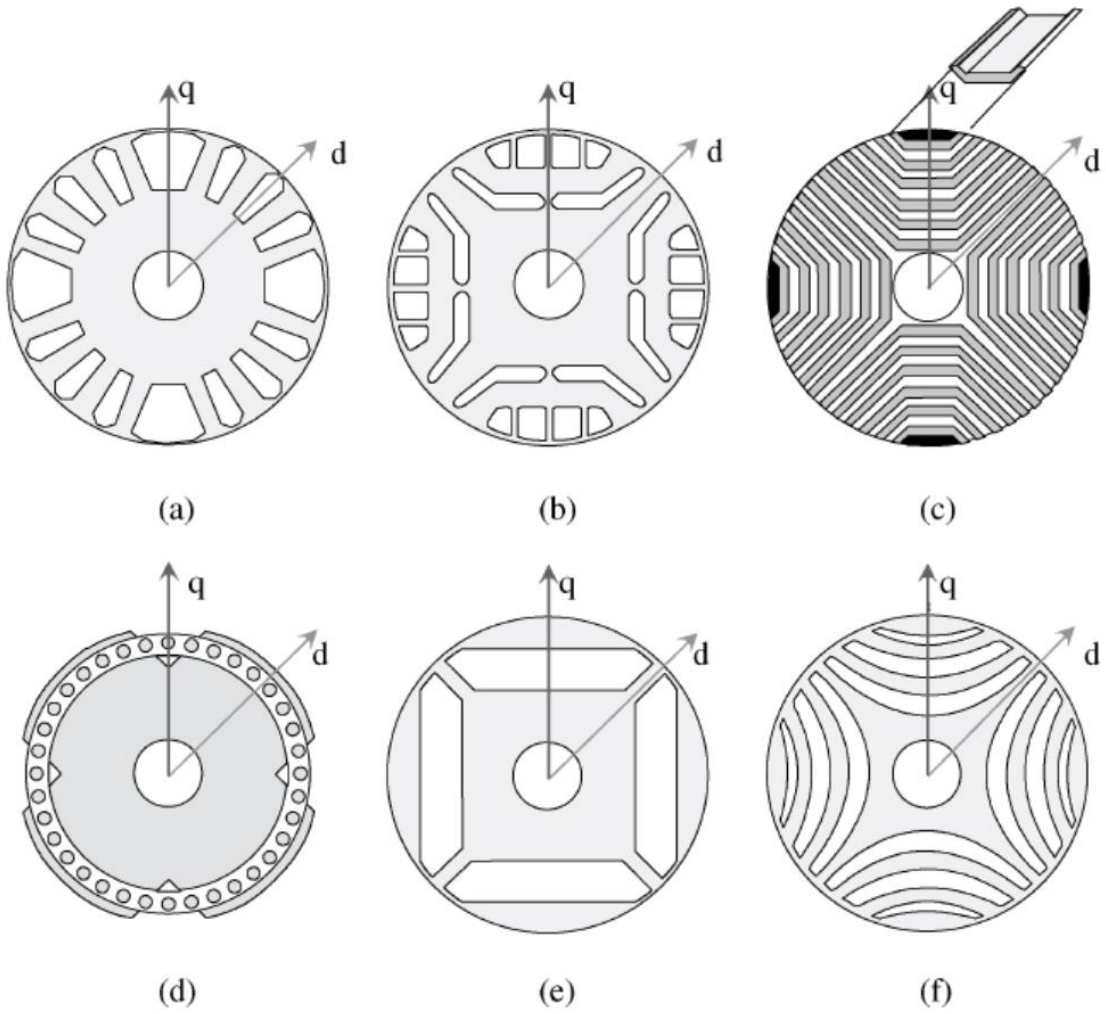


***Figure 21.*** *Possible rotor constructs for synchronous reluctance machine. (a) induction machine rotor with some teeth removed, (b) flux barrier rotor with cage, (c) axially laminated rotor, (d) salient-pole synchronous machine rotor without excitation windings (e) flux barrier rotor without cage and (f) multilayer flux-barrier rotor.[1]*

A simple way to create the rotor for this type of machine is to modify an existing rotor of an induction machine by removing some of its teeth. This type of rotor is displayed in Figure 21 (a). Modifying the rotor of an induction machine is also how the first synchronous reluctance machines were made in the early 1900s. The rotor of a salient pole machine is presented in Figure 21 (d), where the excitation windings have been removed.[1]

In Figure 21 rotors (b) and (e) take advantage of permanent magnets and are referred to as permanent magnet assisted synchronous reluctance machines. The rotor (b) also has a cage winding. These magnets need to be placed in way so that their magnetic

field opposes the q-axis, thus increasing the saliency of the machine. The use of permanent magnets increases the power factor of the machine, which allows the machine to be driven with a less powerful and expensive inverter. Also, permanent magnets increase the energy efficiency of the machine. However, permanent magnets have their downsides. These magnets use rare earth materials, that would noticeably increase the price of the machine. Ferrites are relatively cheap permanent magnets that could be used to make the machine more economical, but to produce the required magnetic field more of these magnets are required, which increases the mechanical strain on the rotor.[1] The maximum speed of the rotor may be also lowered, since the permanent magnets run the risk of separating from the rotor in high-speed applications and high temperature operations run the risk of demagnetizing the magnets[10].

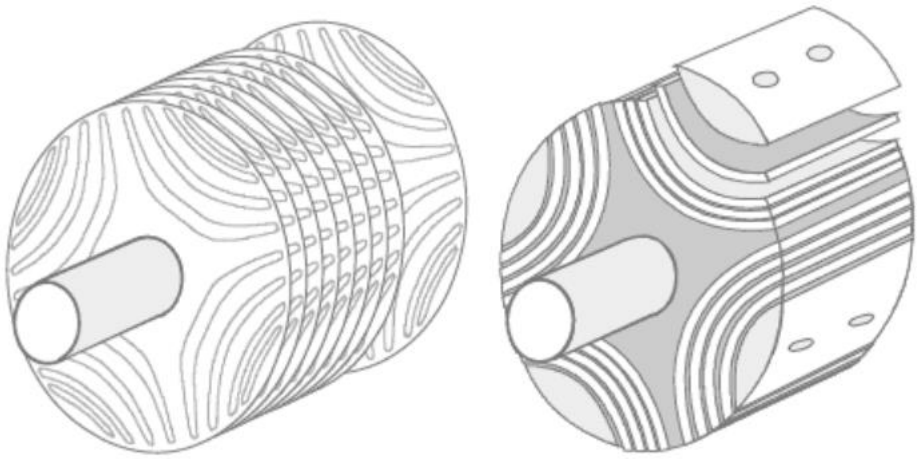

***Figure 22.*** *Transversally- and axially laminated SynRM rotor.[11]*

To increase the efficiency and torque of the SynRM, more suitable rotors have been developed and these modern designs are presented in Figure 21 in rotors (c) and (f). These rotors are called axially- and transversally laminated rotors. Figure 22 displays how the rotor laminations are assembled. It has been determined that the axially laminated rotor is capable of producing more torque with a better power factor, but the rotor construction is more complicated, thus more expensive. The transversally laminated rotor could be produced with similar machinery than the squirrel cage induction machines are produced.[11] It is also possible for the SynRM with this type of rotor to have even

lower production cost than the squirrel cage induction machine, since the cage isn't needed and the casting stage can be skipped in the production line[13].

## 5.2 Operational Principles

The synchronous reluctance machine relies on the principle of the magnetic field's tendency to flow through the points of least reluctance using the least amount of energy. If an object with more reluctance hindering the magnetic field can move so the magnetic field flows with the least amount of energy, torque is generated so the object is moved to align with the field to reduce reluctance. Torque is produced until this position of least reluctance is achieved.[10] SynRM produces torque by constantly maintaining this situation with a rotating magnetic field in the air gap. Opposed to the induction machine, the SynRM rotor rotates at a synchronous speed as its name suggests.

Unlike for the induction machine, the direction with the highest inductance is defined as the d-axis for the synchronous reluctance machine. While designing synchronous reluctance machines it is important to consider the d- and q-axis inductances. The relation between these variables is called the saliency ratio and it is expressed by dividing d-axis inductance with q-axis inductance $L_\mathrm{d}/L_\mathrm{q}$. In Figure 21 different SynRM rotor designs were presented and each of these designs have a different saliency ratio. Rotor (a) has a low saliency of below 3 and rotor (b) and (d) are in between 3 and 4. The more developed rotor designs (c) and (f) have higher saliency ratios of greater than 10 for (c) and from 6 to 8 for (f). It has been determined that the saliency ratio should be at least 6 for SynRM to be capable competing with induction machine.[1]

Produced power can be calculated with

$$P = 3u_\mathrm{s}^2 \frac{L_\mathrm{d} - L_\mathrm{q}}{2\omega_\mathrm{s} L_\mathrm{d} L_\mathrm{q}} \sin 2\delta_\mathrm{s} \tag{49}$$

where $u_s$ is the stator phase voltage, $\omega_s$ is the synchronous rotation speed and $\delta_s$ is the load angle. Load angle is defined as the angle between the stator flux linkage vector and the d-axis. Electrical torque can be expressed with

$$T_e = \frac{3}{2}p\left(L_d - L_q\right)i_{sd}i_{sq} \tag{50}$$

It can be seen from Equations (49) and (50) that they receive greater values the greater the difference of $L_d$ to $L_q$ is. Voltage equations for d- and q-axis can be expressed with [1]

$$u_d = R_s i_{sd} + \frac{d\Psi_d}{dt} - \omega_r \Psi_q \tag{51}$$

$$u_q = R_s i_{sq} + \frac{d\Psi_q}{dt} + \omega_r \Psi_d \tag{52}$$

Earlier presented flux linkage components can be presented with d- and q-axis currents and inductances

$$\Psi_d = L_d i_{sd} = (L_{md} + L_{s\sigma})i_{sd} + L_{md} i_D \tag{53}$$

$$\Psi_q = L_q i_{sq} = \left(L_{mq} + L_{s\sigma}\right)i_{sq} + L_{md} i_Q \tag{54}$$

where $L_{md}$ is magnetizing inductance in d-axis, $L_{mq}$ is magnetizing inductance in q-axis, $L_{s\sigma}$ is stator leakage inductance, $i_D$ is damper winding current in d-axis and $i_Q$ is damper winding current in q-axis. With these earlier presented 4 equations an equivalent circuit can be formed in d- and q-axis, that is shown in Figure 23.[1]

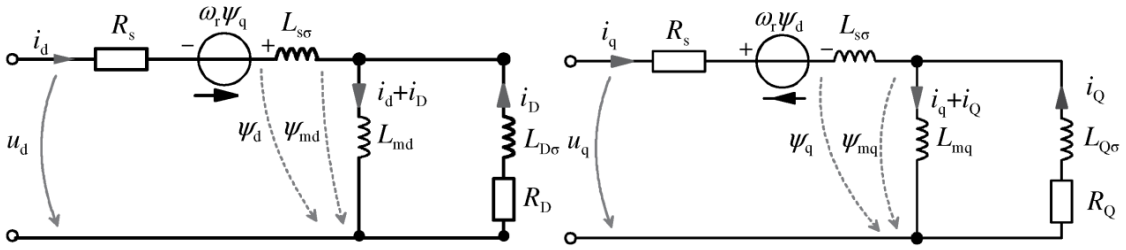


***Figure 23.*** *Equivalent circuit of synchronous reluctance machine with damper winding in d- and q-axis presentation.[1]*

Figure 23 is modelled with a damper winding, which allows the SynRM to be operated directly from the grid without a frequency converter. This is called direct online (DOL) use. The damper winding, however, reduces the saliency ratio of the machine and direct online use doesn't allow variable speed operations. If the SynRM is operated with a frequency converter, damper winding can be removed to increase the efficiency of the machine, as no rotor currents are produced.[1] By removing these windings, the Equations (53) and (54) and Figure 23 are also simplified as the terms relating to damper winding can be removed.

Stator flux linkage vector can be formed with

$$\boldsymbol{\Psi}_\mathrm{s} = \boldsymbol{\Psi}_{\mathrm{s}\sigma} + \boldsymbol{\Psi}_\mathrm{m} \tag{55}$$

where $\boldsymbol{\Psi}_{\mathrm{s}\sigma}$ is stator leakage flux linkage vector and $\boldsymbol{\Psi}_\mathrm{m}$ is air gap flux linkage vector.[1]

Equations (53) and (54) and $i_{\mathrm{sd}}$ and $i_{\mathrm{sq}}$ can be presented in relation to the load angle $\delta_\mathrm{s}$ by

$$\Psi_\mathrm{d} = \Psi_\mathrm{s}\cos\delta_\mathrm{s} = \Psi_\mathrm{m}\cos\delta_\mathrm{s} + i_{\mathrm{sd}}L_{\mathrm{s}\sigma} \tag{56}$$

$$\Psi_\mathrm{q} = \Psi_\mathrm{s}\sin\delta_\mathrm{s} = \Psi_\mathrm{m}\sin\delta_\mathrm{s} + i_{\mathrm{sq}}L_{\mathrm{s}\sigma} \tag{57}$$

$$i_{\mathrm{sd}} = \frac{1}{L_\mathrm{d}}\Psi_\mathrm{s}\cos\delta_\mathrm{s} \tag{58}$$

$$i_{\mathrm{sq}} = \frac{1}{L_\mathrm{q}}\Psi_\mathrm{s}\sin\delta_\mathrm{s} \tag{59}$$

and a visual space vector presentation of all of these values is presented in Figure 24.[1] Figure 24 also displays phase angle $\varphi$, current angle $\kappa$ and rotor angle $\theta_r$.

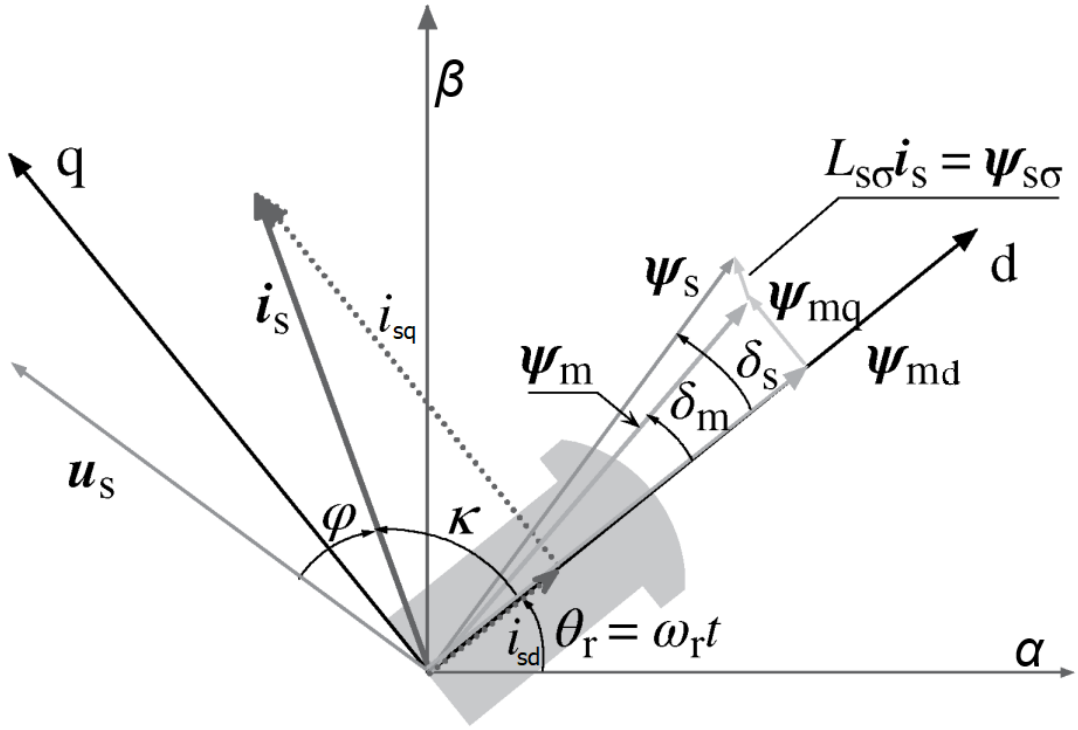


***Figure 24.*** *Space vector presentation of SynRM variables. Modified from [1].*

High saliency ratio is preferable for high torque and power factor, and better torque response, but there are limits how much a higher saliency ratio improves the operation of the SynRM. Figure 25 presents 3 curves for break-down torque with different saliency ratios, which display its effect on torque, and the effect of the load angle. The motor was driven at rated voltage and frequency. It can be seen from this figure that the maximum torque is produced at the load angle of 45°, and the increase in the saliency ratio from 10 to 50 is less significant than the increase from 5 to 10 for the break-down torque. Saliency ratio of 50 is considered practically non achievable, but its curve in Figure 25 presents, that the increase in the saliency ratio has lower improvements in break-down torque after high enough saliency has been achieved. These values are produced with equation

$$T_e = \frac{1 - \frac{1}{L_d/L_q}}{2L_q} \sin 2\delta_s \quad (60)$$

where $L_d$ is the d-axis inductance and $\delta_s$ is the load angle.[1]

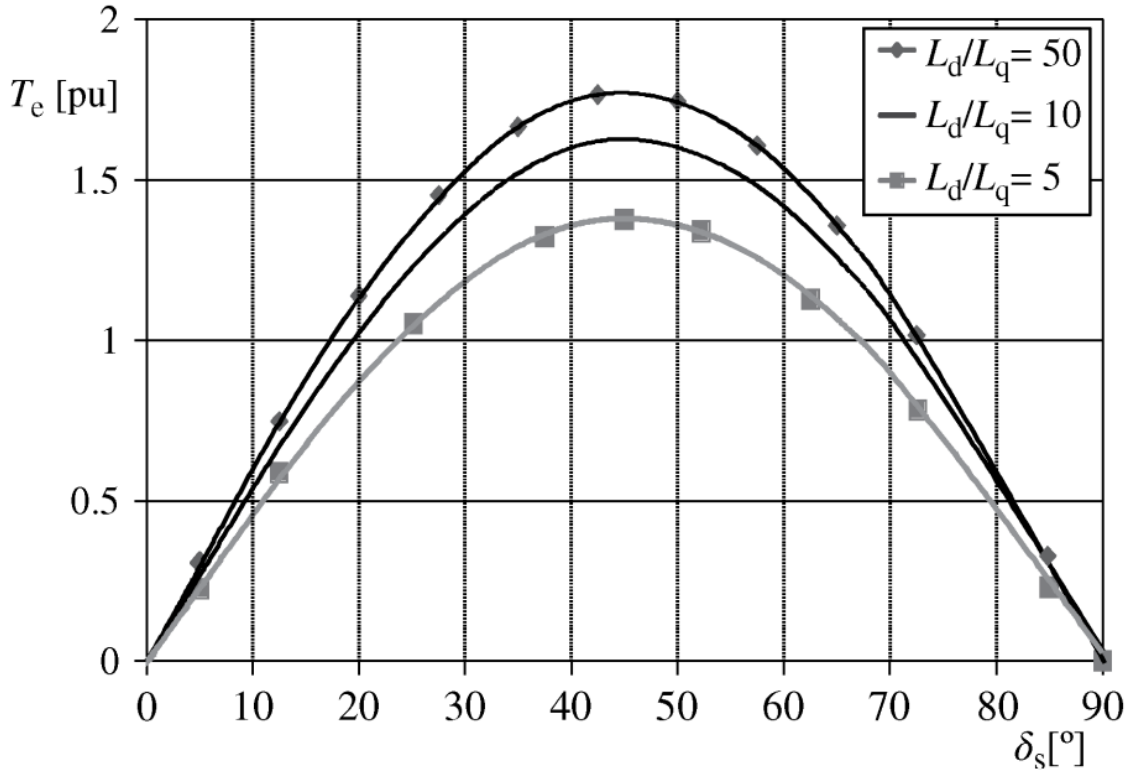


***Figure 25.*** *Different break-down torques for different saliency ratios in SynRM with $L_q$=0,27.[1]*

The power factor is one parameter that has been compared with the induction machine, and generally for the synchronous reluctance machine it is lower. Higher saliency can improve it while a proper load angle is selected. Figure 26 displays the effect of saliency and the load angle on the power factor. Increasing saliency ratio improves power factor more significantly, when compared with how in Figure 25 break-down torque improved with better saliency ratio.[1]

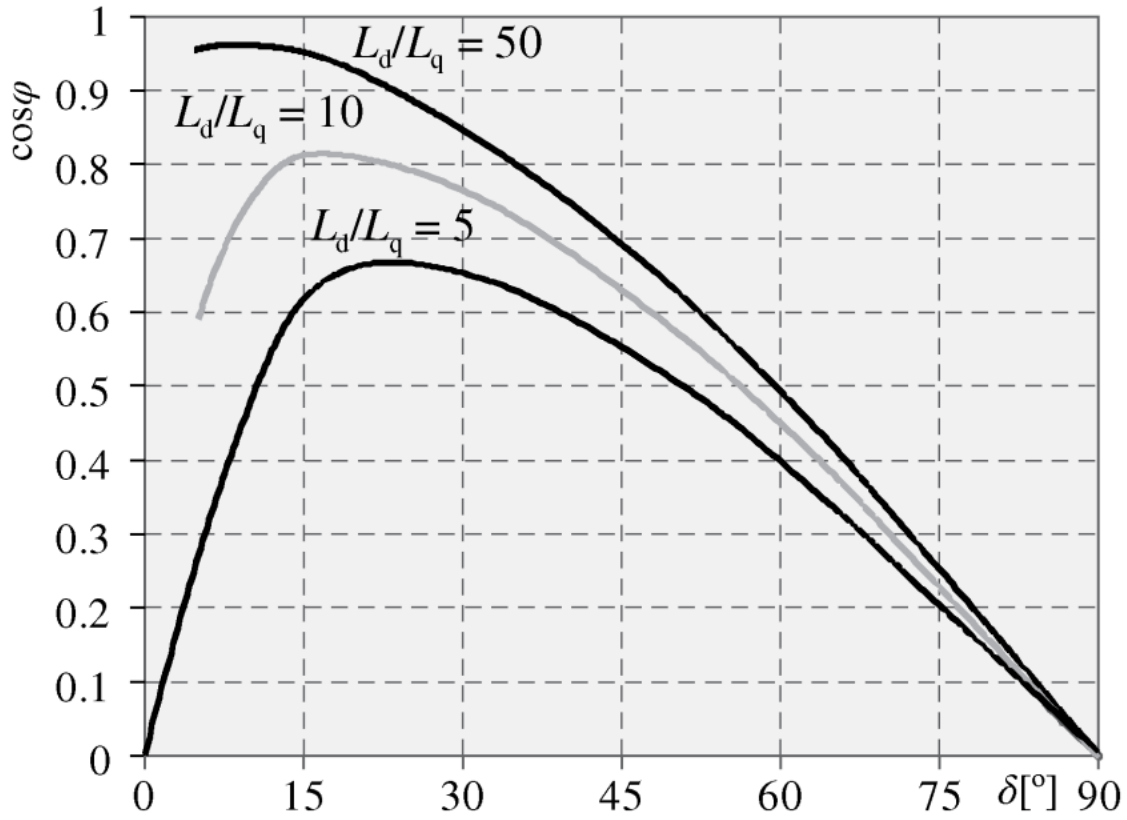


***Figure 26.*** *SynRM power factor with different saliency ratios.[1]*

## 5.3 Motor Control

The synchronous reluctance machine is usually controlled with a vector control method, that is implemented with either field-oriented control or direct torque control (DTC). For this chapter, the field-oriented control is prioritized and no other motor control methods are considered. Since the principles of FOC were introduced in Chapter 4.3.3, this chapter aims to mainly present different versions of field-oriented control for the SynRM.

### 5.3.1 Field-oriented control (FOC)

Synchronous reluctance machine uses the same principles for field-oriented control as the induction machine presented in Chapter 4.3.3, but with some adjustments due to dissimilarities in the operational principles of the machines. Stator current is again divided into d- and q-components, where current $i_{sd}$ is used to control the excitation flux and $i_{sq}$ controls torque. Figure 27 displays a block diagram of this control. In this figure

$\omega_{ref}$ is speed reference and $u_{Uref}$, $u_{Vref}$ and $u_{Wref}$ are voltage references sent to the inverter of the frequency converter.

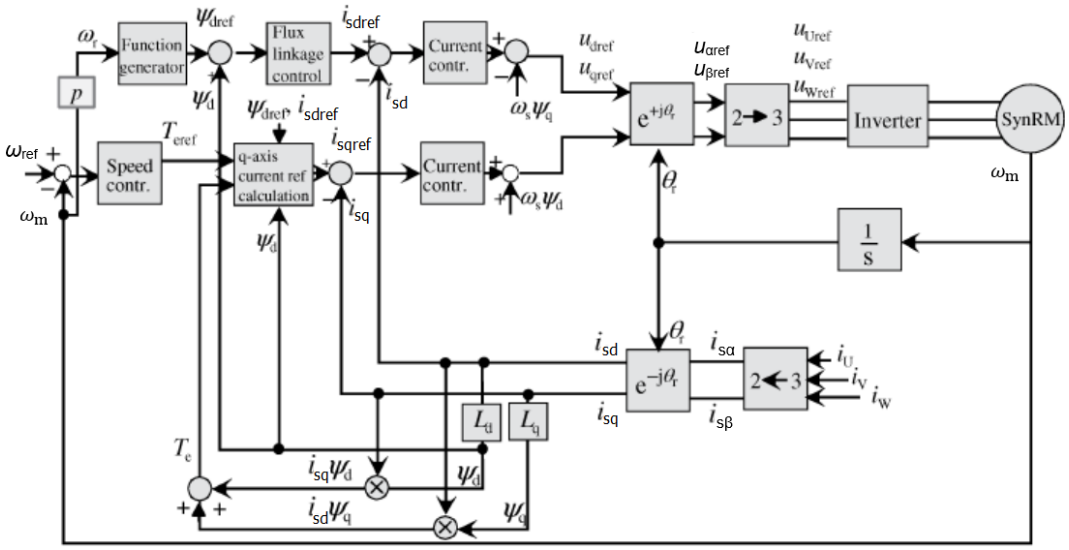


***Figure 27.*** *SynRM block diagram for field-oriented control, modified from[1].*

There are different methods how to implement this control, based on what is the most desired feature for the control. These methods can be divided into two: constant $i_{sd}$ control and constant current angle $\kappa$ control. Constant current angle control can be further divided into the fastest torque response control, maximum torque per ampere (MTPA) control and maximum power factor control. Constant $i_{sd}$ control is best used for cases, where motor is driven outside of the field weakening region.[1]

## 5.3.2 Constant $i_{sd}$ control

As the name implies, constant $i_{sd}$ control maintains certain $i_{sd}$ value in operations below rated frequency. To get the current control equations, first the stator flux equation needs to be examined, which is presented by

$$\Psi_s = \sqrt{\Psi_d^2 + \Psi_q^2} = \sqrt{(L_d i_{sd})^2 + \left(L_q i_{sq}\right)^2} \tag{61}$$

current $i_{sq}$ can be solved from this equation by

$$i_{sq} = \frac{\sqrt{\Psi_s^2 - (L_d i_{sd})^2}}{L_q} \tag{62}$$

Torque equation for the SynRM was presented in Equation (56). If $i_{sq}$ from Equation (62) is inserted here, the equation takes form

$$T_e = \frac{3}{2}\frac{p}{L_q}\left(L_d - L_q\right)i_{sd}\sqrt{\Psi_s^2 - (L_d i_{sd})^2} = \frac{3}{2}p\left(\frac{L_d}{L_q} - 1\right)i_{sd}\sqrt{\Psi_s^2 - (L_d i_{sd})^2} \quad (63)$$

Current $i_{sd}$ can be solved from Equation (69) by partially deriving it by $i_{sd}$ and solving it for zero, which produces

$$i_{sd} = \frac{\Psi_s}{\sqrt{2}L_d} \quad (64)$$

This equation can be used for reference values for $i_{sd}$. Maximum torque can be defined as

$$T_{emax} = \frac{3}{4}p\frac{L_d - L_q}{L_d L_q}\Psi_s^2 = \frac{3}{4}p\left(\frac{1}{L_q} - \frac{1}{L_d}\right)\Psi_s^2 \quad (65)$$

Using this equation, the maximum value for stator flux linkage can be presented as

$$\Psi_{smaxref} = \sqrt{\frac{4|T_{eref}|L_d L_q}{3p\left(L_d - L_q\right)}} \quad (66)$$

The stator flux linkage reference defined here can be inserted into Equation (64) to get the current reference for maximum torque. Finally, the reference value for $i_{sq}$ is defined as

$$i_{sqref} = \frac{2T_{eref}}{3p\left(L_d - L_q\right)i_{dref}} \quad (67)$$

where the subscript ref refers the value being a reference value.[1]

### 5.3.3 Fastest torque response

The 3 constant $\kappa$ control strategies all depend on tan $\kappa$. To solve the fastest torque response situation, first the $i_{sq}$ is solved from Equation (63) by partially deriving it by $i_{sq}$ and solving it for zero, which produces

$$i_{\mathrm{sq}} = \frac{\Psi_{\mathrm{s}}}{\sqrt{2}L_{\mathrm{q}}} \tag{68}$$

dividing Equation (68) with Equation (64) produces

$$\frac{i_{\mathrm{sq}}}{i_{\mathrm{sd}}} = \frac{\frac{\Psi_{\mathrm{s}}}{\sqrt{2}L_{\mathrm{q}}}}{\frac{\Psi_{\mathrm{s}}}{\sqrt{2}L_{\mathrm{d}}}} = \frac{L_{\mathrm{d}}}{L_{\mathrm{q}}} \tag{69}$$

which is equal to tan $\kappa$. From this equation, the angle for the highest rate of change for torque can be defined by

$$\kappa = arctan\frac{L_{\mathrm{d}}}{L_{\mathrm{q}}} \tag{70}$$

Solving stator flux linkage from Equation (64) and inserting it into Equation (65), reference for $i_{\mathrm{sd}}$ can be solved by

$$\Psi_{\mathrm{smaxref}} = i_{\mathrm{sdref}}\sqrt{2}L_{\mathrm{d}} \tag{71}$$

$$i_{\mathrm{sdref}} = \frac{\sqrt{\frac{4|T_{\mathrm{eref}}|L_{\mathrm{d}}L_{\mathrm{q}}}{3p(L_{\mathrm{d}}-L_{\mathrm{q}})}}}{\sqrt{2}L_{\mathrm{d}}} = \sqrt{\frac{4|T_{\mathrm{eref}}|L_{\mathrm{d}}L_{\mathrm{q}}}{3p(L_{\mathrm{d}}-L_{\mathrm{q}})2L_{\mathrm{d}}^2}} = \sqrt{\frac{2|T_{\mathrm{eref}}|L_{\mathrm{q}}}{3p(L_{\mathrm{d}}-L_{\mathrm{q}})L_{\mathrm{d}}}} \tag{72}$$

this equation can be changed to take into account tan $\kappa$, which produces

$$i_{\mathrm{sdref}} = \sqrt{\frac{2|T_{\mathrm{eref}}|}{3p(L_{\mathrm{d}}-L_{\mathrm{q}})\tan\kappa}} \tag{73}$$

Considering Equations (70) and (71), the reference value for current $i_{\mathrm{sq}}$ can be defined as

$$i_{\mathrm{sqref}} = \frac{i_{\mathrm{sdref}}sgn(T_{\mathrm{eref}})}{\tan\kappa} \tag{74}$$

where the sgn() function produces either a positive or negative sign depending on the sign of the torque reference.[1]

### 5.3.4 Maximum torque per ampere (MTPA)

When Equation (50) displaying torque is modified to depend on the current angle $\kappa$ and the stator current $i_s$, the equation is expressed as

$$T_\mathrm{e} = \frac{3}{4} p i_\mathrm{s}^2 \left(L_\mathrm{d} - L_\mathrm{q}\right) \sin 2\kappa \tag{75}$$

It can be clearly seen from this equation, that the maximum value is achieved when $\kappa$ is π/4, which produces the MTPA condition.[1]

### 5.3.5 Maximum power factor

To get the maximum power factor for the SynRM, first the equation for power factor is presented as

$$\cos\varphi = \frac{2T_\mathrm{e}\omega_\mathrm{s}}{3pu_\mathrm{s}i_\mathrm{s}} \tag{76}$$

Next, the equations for stator voltage and stator current can be presented as

$$u_\mathrm{s} = \omega_\mathrm{s}\Psi_\mathrm{s} \tag{77}$$

$$i_\mathrm{s} = \sqrt{i_\mathrm{sd}^2 + i_\mathrm{sq}^2} \tag{78}$$

When torque Equation (50) and the two earlier equations are inserted into the power factor Equation (76), the power factor can be solved with

$$\cos\varphi = \frac{\left(L_\mathrm{d} - L_\mathrm{q}\right) i_\mathrm{sd} i_\mathrm{sq}}{\sqrt{\left(L_\mathrm{d} i_\mathrm{sd}\right)^2 + \left(L_\mathrm{q} i_\mathrm{sq}\right)^2}\sqrt{i_\mathrm{sd}^2 + i_\mathrm{sq}^2}} \tag{79}$$

This new equation is then differentiated in respect to $i_{sd}/i_{sq}$ and solved for zero, which produces a condition for maximum power factor

$$\frac{i_\mathrm{sq}}{i_\mathrm{sd}} = \sqrt{\frac{L_\mathrm{d}}{L_\mathrm{q}}} \tag{80}$$

The relation between $i_{sq}/i_{sd}$ and tan $\kappa$ was expressed in Equation (69). Considering this, the current angle for maximum power factor can be defined with equation

$$\kappa = arctan\sqrt{\frac{L_{\mathrm{d}}}{L_{\mathrm{q}}}} \tag{81}$$

which produces the constant $\kappa$ condition for maximum power factor.[1]

# 6. ELECTRICAL MACHINE LOSSES

Electrical machines perform electro-mechanical power conversion. The direction of this operation is determined whether the machine is used as a motor or a generator, implying that electrical power is used to produce mechanical power or mechanical power is used to generate electrical power. These operations are not perfect and losses are generated due to different phenomena. Power losses that occur in an electrical machine can be divided into following 4 categories:

1. copper losses
2. core losses
3. mechanical losses
4. stray losses.

Figure 28 visualizes and divides these losses for stator and rotor. Arrow sizes in this figure do not represent the magnitudes of actual losses an electrical machine produces.

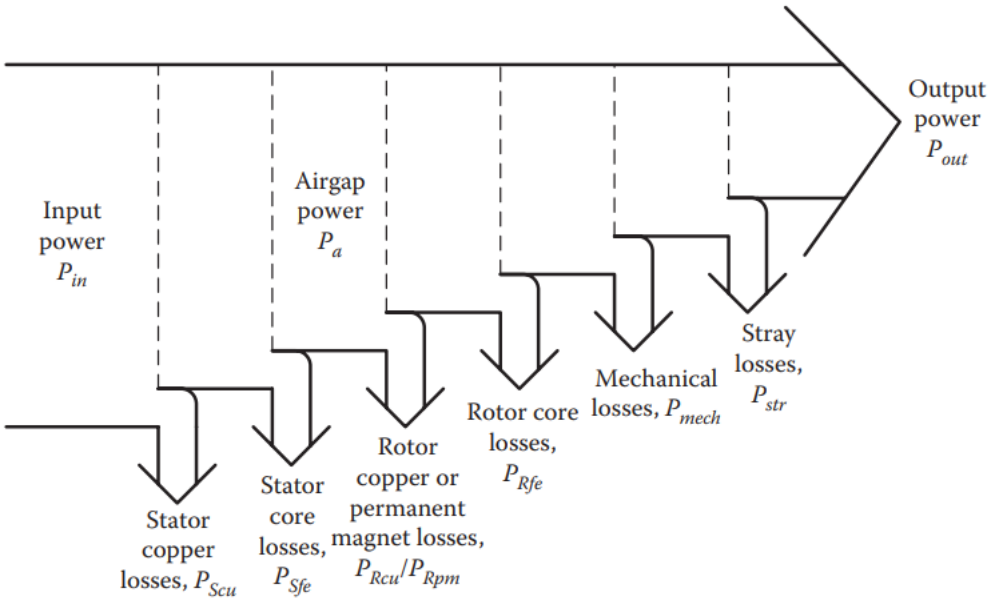


***Figure 28.*** *General losses of an electrical motor, modified from[10].*

## 6.1 Copper losses

Copper losses, also known as resistive losses, occur in current carrying conductors, which increases the temperature of the conductor. These losses can be determined with basic power and voltage equations as

$$P_{cu} = ui = (iR)i = i^2R \tag{82}$$

where *R* is the resistance of the conductor. This equation can be modified to present these loses using current density and its surface area, while expressing resistance with resistivity and conductor's length by

$$P_{cu} = i^2R = i^2\rho\frac{l}{S} = (JS)^2\rho\frac{l}{S} = 2\pi l\rho\int_0^{r_0} J^2(r)rdr \tag{83}$$

where $\rho$ is resistivity of the conductor, *l* is the length of the conductor, *S* is the surface area of the conductor, *J* is the current density and *r* the radius of a round conductor. Current distribution in a conductor is homogenous with DC-current, but when operated with AC-currents, this distribution changes in relation to the frequency. This effect is called skin effect, which directs more current to flow on the surface of the conductor than in its center. Uneven current distribution causes more copper losses. Skin effect is

caused by eddy currents, which are discussed in the core losses section. Figure 29 displays how skin effect can change the current distribution.[10]

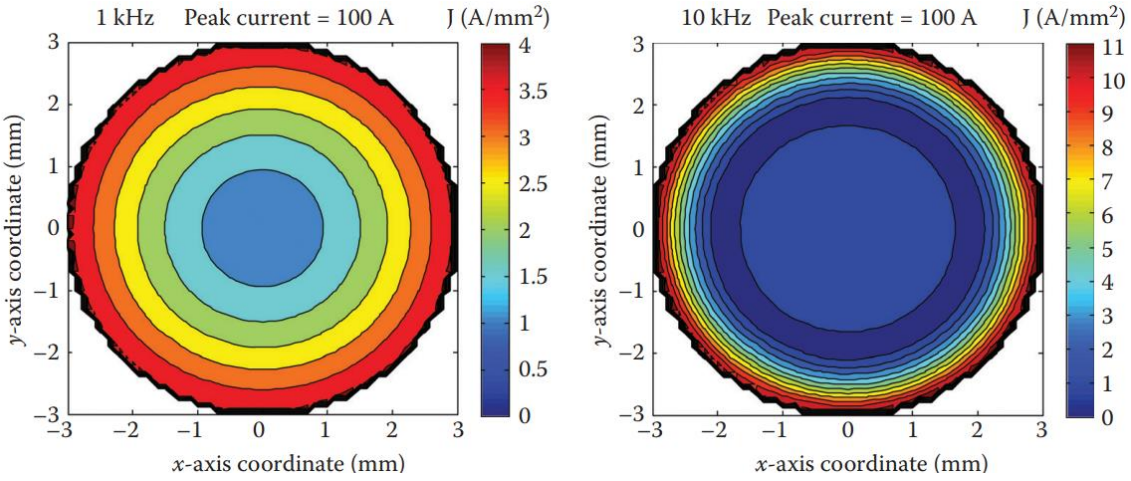


***Figure 29.*** *Skin effect on a conductor with different frequencies.[10]*

It is also possible for eddy current from other conductors to change the current distribution, which causes an effect called proximity effect. This effect is more significant as the frequency increases. Figure 30 depicts this effect.[10]

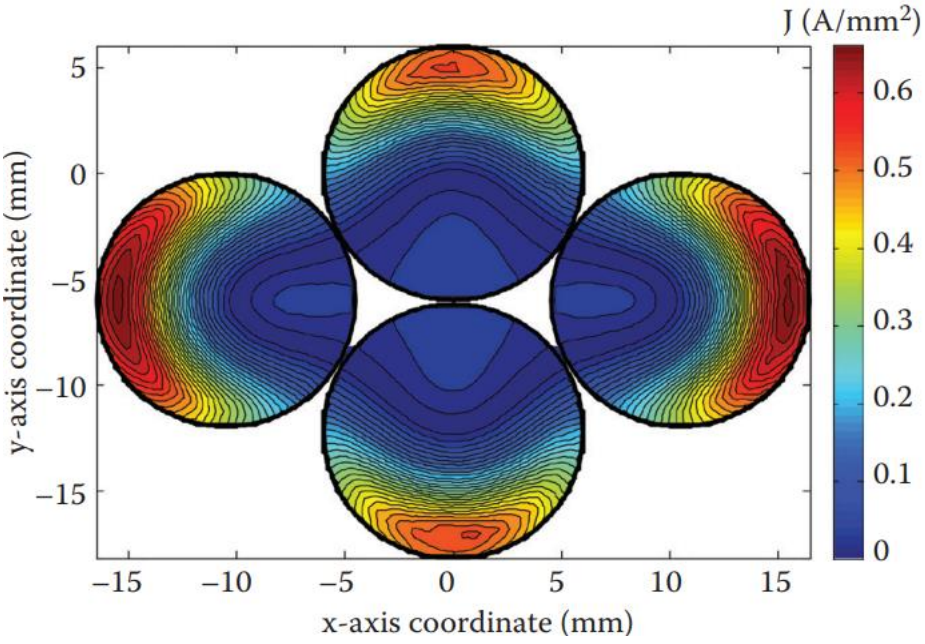


***Figure 30.*** *Proximity effect on a conductor.[10]*

## 6.2 Core losses

Core losses, or iron losses, of an electrical machine are caused by alternating flux in the machine. These losses can occur when the machine experiences transients. Core losses can be divided into eddy current losses and hysteresis losses.[11]

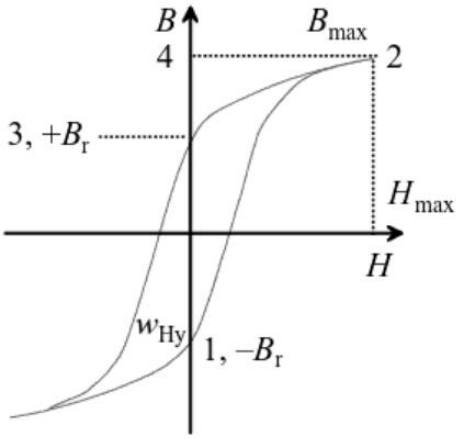


***Figure 31.*** *Hysteresis loop in a magnetic circuit.[11]*

When a magnetic field is applied to the core, the magnetic dipoles in the material are subjected to torque from the external field, which causes these dipoles to align parallel to the applied field. The stronger the magnetic field, the more aligned the dipoles become. When all the dipoles have fully aligned with the magnetic field, the material is considered saturated, which produces a limit for the maximum achievable magnetic field in the core. The material is magnetized and demagnetized in use, and this periodic change can be presented with a hysteresis loop. This loop is presented in Figure 31. The area under hysteresis loop is used to magnetize the material and expended as heat, This loss is called hysteresis loss.[10]

Alternating flux induces voltages in the conductive material. This fluctuation creates eddy currents, which resist the changes in magnetic flux. Eddy currents in a solid material can become enormous, which would prevent the flux from penetrating the material. A common method to reduce the effects of eddy currents, and the losses they cause, is to build the object from multiple thin laminations or use high resistivity compound materials.[11]

## 6.3 Mechanical losses

Mechanical losses in electrical machines occur in form of friction between air and rotating parts of the machine, which causes the temperature to increase. This friction loss can be divided between bearing- and windage losses. Magnitudes of these losses depend on the mechanical design of the machine and the speed the machines are operated at. Speed affects windage losses more significantly, which is displayed in Figure 32.[10], [11]

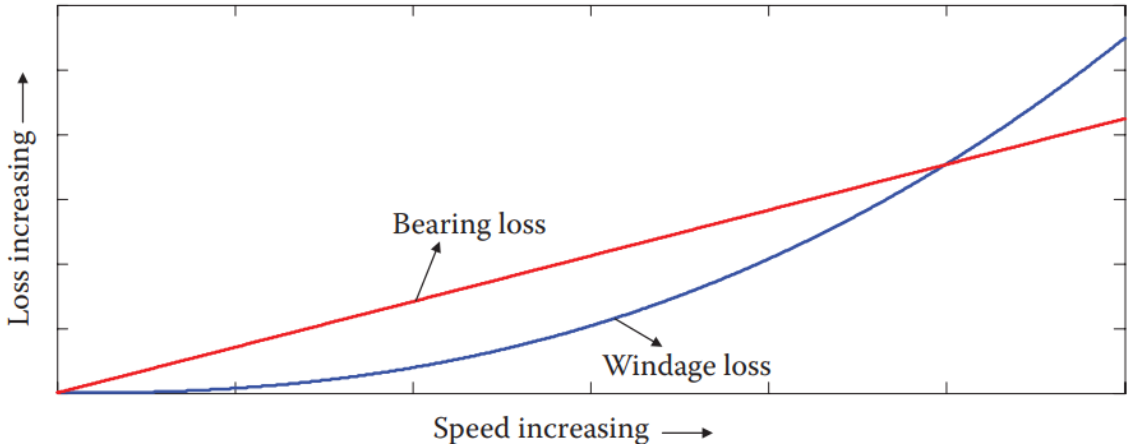


***Figure 32.*** *Bearing and windage losses as speed increases.[10]*

## 6.4 Stray losses

Stray losses, or additional losses, are defined by how they are not part of the earlier mentioned three losses. IEC standard 60034-2-1 “Standard methods for determining losses and efficiency from tests” can be used to calculate these losses by first measuring the total losses and then measuring the copper-, core- and mechanical losses, all of these according to the mentioned standard. The difference in total losses and the sum of the earlier mentioned three losses is defined as stray losses. Table 1 displays stray loss percentages of input power for different electrical machines.[11]

**Table 1.** *Stray losses in different electrical machines[11].*

| Machine type | Additional losses of input power |
|---|---|
| Squirrel cage motor | 0,3-2 % (sometimes up to 5%) |
| Slip-ring asynchronous machine | 0,5 % |
| Salient-pole synchronous machine | 0,1-0,2 % |
| Nonsalient-pole synchronous machine | 0,05-0,15 % |
| DC-machine without compensating winding | 1 % |
| DC-machine with compensating winding | 0,5 % |

# 7. EVALUATION OF INDUCTION MACHINE AND SYNCHRONOUS RELUCTANCE MACHINE

In this chapter, induction machine and synchronous reluctance machine are compared with each other while also considering their suitability for crane applications. This comparison is done by evaluating torque production, field-weakening capabilities, and energy efficiency. Many comparative studies have been conducted between these electrical machines, for example studies [14]–[20]. The general conclusion of these studies is that synchronous reluctance machine is more energy efficient but has a lower power factor. One popular application for comparisons for these motors has been the traction applications.

## 7.1 Crane application requirements

The capability for flux braking for an electrical machine is considered beneficial. With this method, the extra generated power can be dissipated by using it to increase magnetization of the machine. For bridge cranes, the horizontal movement needs to be also considered. Two motors are placed on the opposite sides of the main girder and they need to move at the same speed. 2 induction machines can be driven with a single frequency converter for this application, but synchronous reluctance machine requires a dedicated frequency converter for each motor. These frequency converters can then be controlled with a programmable logic controller (PLC) that monitors the speed of the motors, so they operate at the same speed. Sensors need to be used for speed monitoring. For field-weakening operations the capability to reach a speed that is multiple times the nominal speed is preferred. When considering torque production, the motor should be capable of operating with a high torque in low-speed regions and the motor should never be operated at the torque limit that is defined for the motor. The motor should be capable of producing at least 150% torque from the nominal. For bigger mo-

tors the capability to stop an uncontrolled falling load is a feature that can be implemented. Efficiency of the motor should be as high as possible. The temperature of the motor needs to be controlled according to the requirements of the different crane applications. There are different duty types for this, which are defined in standard IEC 60034-1. Motor control should be capable of handling operations in cold and hot temperatures. It is also a positive feature if the inherent parameters of the electrical machine can be easily discovered with a frequency converter.[21]

In addition to requirements mentioned above, capability to follow speed commands accurately is also a feature, which is considered beneficial. Also, motor control should be capable of maintaining control during sudden changes in load torque.

## 7.2 Torque production

The main purpose of an electric motor is to produce torque, which is then applied to different loads to realize different applications. It is thus important to evaluate torque production capabilities, when two different electrical machines are compared with each other. Torque equation for induction machine in dq-reference frame was presented in Chapter 4.3.1 using flux linkage terms, but this equation can be simplified and made more similar to how the equation was for synchronous reluctance machine by [22]

$$T_{e,IM} = \frac{3}{2} p \frac{L_m^2}{L_r} i_{\mathrm{sd}} i_{\mathrm{sq}} \tag{84}$$

where $L_\mathrm{m}$ is the magnetizing inductance and $L_\mathrm{r}$ is the rotor self-inductance. It can be seen that the only difference in this equation to the SynRM torque Equation (50) is the inductance term.

Break-down torque for the synchronous reluctance machine was presented in Figure 25, which displays that this torque can be quite low, around 150% of the nominal torque. For the induction machine, the break-down torque is around 300%[1]. This re-

veals one significant difference between these electrical machines. For some applications higher torque range is required, which might completely remove the synchronous reluctance machine as an option. However, these break-down torques are defined with nominal values. Electrical machines can be overloaded, which causes the machine to intake more current, but produce more torque[13]. This will, however, further increase the temperature of the machine, which will limit the use of the machine. If a temperature limit is defined for torque production that the electrical machine is not allowed to cross, this could offer the SynRM opportunities as an alternative for the induction machine. An experimental study[16] has been conducted, which presents that the transversally laminated synchronous reluctance machine (TLSynRM) has better thermal properties than the induction machine, which allows the machine to produce more torque. The results of this study are displayed in Table 2, which presents results for motors with the nominal voltage of 400 V and the nominal power of 4 kW.

**Table 2.** *Comparison of induction machine and TLSynRM.[16]*

| | IM | TLSynRM (equal torque) | TLSynRM (equal temperature) |
|---|---|---|---|
| T (Nm) | 27,1 | 27,1 | 31,7 |
| $n_s$ (rpm) | 1202 | 1100 | 1100 |
| $n_r$ (rpm) | 1101 | 1100 | 1100 |
| av. winding temperature (°C) | 104 | 80 | 108 |
| $u_{rms}$ (V) | 323 | 305 | 317 |
| $i_{rms}$ (A) | 8,63 | 9,56 | 10,8 |
| $P_{in}$ (W) | 4050 | 3750 | 4480 |
| $P_{out}$ (W) | 3125 | 3122 | 3652 |
| Efficiency | 0,772 | 0,832 | 0,815 |
| Fundamental power factor | 0,839 | 0,743 | 0,756 |
| $P_{jstat}$ (W) | 442 | 508 | 705 |
| $P_{jrot}$ (W) | 295 | 0 | 0 |
| $P_{loss}$ (W) | 925 | 628 | 828 |
| $P_{in}$-$P_{out}$-$P_{js}$-$P_{jr}$ | 189 | 120 | 123 |

Table 2 shows that the SynRM has higher efficiency, but a lower power factor in both test cases. The SynRM is capable of producing more torque than the induction machine when a temperature limit is defined and both of these machines are operated continuously at this temperature. Lower power factor cause higher currents for the synchronous reluctance machine, which lead to higher stator losses. It should be noted that the SynRM needs more current due to the lower power factor, which might require a bigger frequency converter when compared with the induction machine. This will be important if the lower break-down torque of the synchronous reluctance machine is improved with overloading.

## 7.3 Field-weakening operation

With field-weakening, electrical machines can operate at higher speeds than their nominal. Speed is normally increased by increasing the voltage, but this only works below nominal speed. To reach higher speeds, the motor control can change the current distribution between the d- and q-axis by increasing the q-portion of the current and lowering the d.

To properly model field-weakening capabilities of an electrical machine, first the voltage and current limits need to be defined. These can be expressed in dq-current plane as circles and ellipses with

$$u_{s,max}^2 \geq u_{sd}^2 + u_{sq}^2 \tag{85}$$

$$i_{s,max}^2 \geq i_{sd}^2 + i_{sq}^2 \tag{86}$$

where $u_{s,max}$ is the maximum voltage and $i_{s,max}$ is the maximum current for the frequency converter. The d- and q-voltage terms in the maximum voltage equation are formed according to the working principles of the electrical machine being modelled.[22], [23]

### 7.3.1 Induction machine

Induction machine voltage equations in steady state can be modelled with

$$u_{sd} = R_s i_{sd} - \omega_e \sigma L_s i_{sq} \tag{87}$$

$$u_{sq} = R_s i_{sq} + \omega_e L_s i_{sd} \tag{88}$$

where σ is leakage coefficient, that is defined as

$$\sigma = 1 - \frac{L_m^2}{L_s L_r} \tag{89}$$

Using Equations (87) and (88), the maximum voltage equation takes form

$$u_{s,max}^2 \geq \left(R_s i_{sd} - \omega_e \sigma L_s i_{sq}\right)^2 + \left(R_s i_{sq} + \omega_e L_s i_{sd}\right)^2 \tag{90}$$

This maximum voltage equation and the maximum current equation can be used to draw a limiting circle and an ellipse for the induction machine, which are displayed in Figure 33. The voltage limit depends on speed. This limit decreases as the speed of the motor is increased. The motor needs to be always operated within these circles.[22]

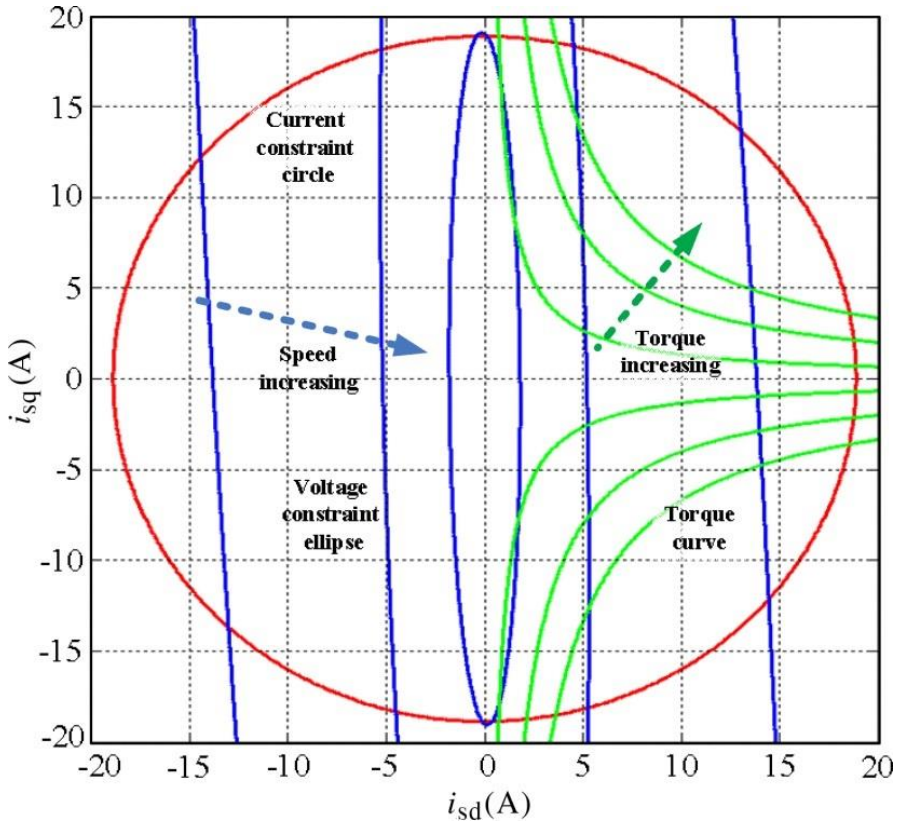


***Figure 33.*** *Current- and voltage limits for induction machine. Modified from [22].*

Field-weakening has two important speed ranges for the induction machine and the first section is displayed in Figure 34. In this figure, field weakening is started from the nominal speed point, which is displayed as the point B. As speed increases, the voltage limit decreases. If the motor is to be operated at maximum torque, the operation should be controlled so the current vector is always kept at the intersection of the current limit circle and the voltage limit ellipse. Speed is increased and the operation follows along the current limit circle until point C is reached, where the field-weakening control changes to follow only the voltage limit ellipse. The maximum value for the q-axis current can be defined with

$$\left|i_{sq,limit1}\right| = \sqrt{i_{s,max}^2 - i_{sd}^2} \tag{91}$$

where current limit $i_{sq,limit1}$ is usable, when the field-weakening operation happens between the points B and C.[22]

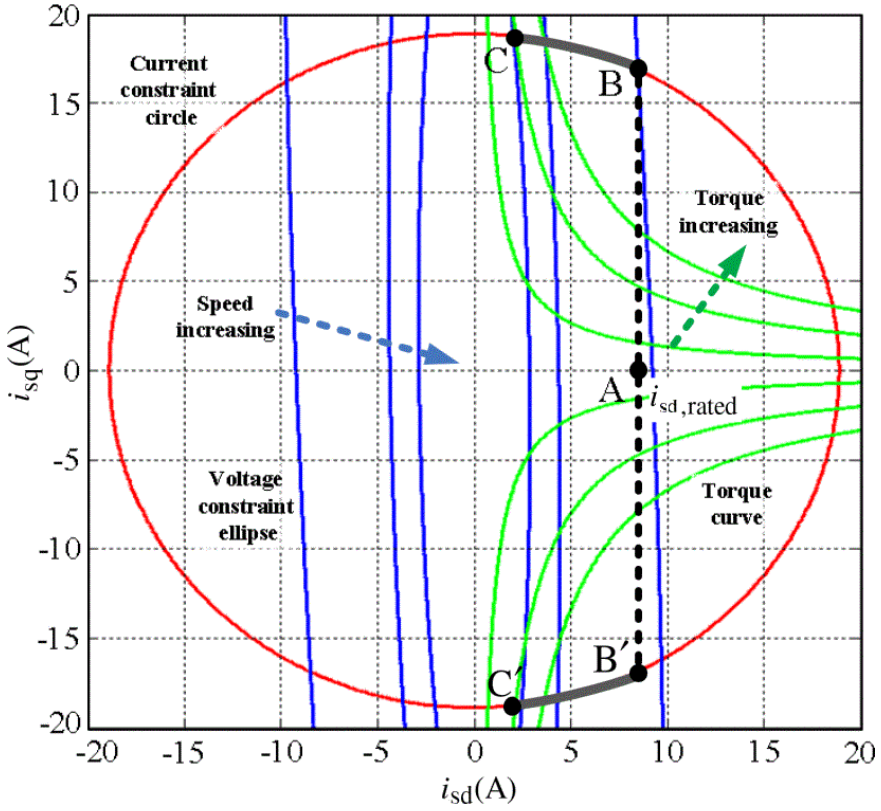


***Figure 34.*** *Induction machine field-weakening operation. Modified from [22].*

When speed is further increased from point C, the voltage limit ellipse continues shrinking and no longer intersects the current limit circle at the angle that corresponds to the speed. Due to this change, the voltage limit ellipse now becomes the main limiting factor for the current. This change is displayed in Figure 35, as the field-weakening continues from point C into point D. In this region the voltage limit equation can be simplified by removing the stator resistance voltage drop and the equation is remodeled into

$$\frac{u_{s,max}^2}{(\sigma L_s \omega_e)^2} \geq i_{sq}^2 + \left(\frac{i_{sd}}{\sigma}\right)^2 \tag{92}$$

This equation is usable as long as $i_{sq}$ is smaller than $i_{sd}/\sigma$. The equation for current limit for q-axis $i_q$ is modified to include rotor flux equation

$$\psi_{rd} = L_m i_{sd} \tag{93}$$

which is then included in the current limit equation

$$\left|i_{sq,limit2}\right| = \frac{\psi_{rd}}{\sigma L_m} \tag{94}$$

Figure 34 and 35 also display operating points B' and C', that are used to present the generator use in field-weakening area.[22]

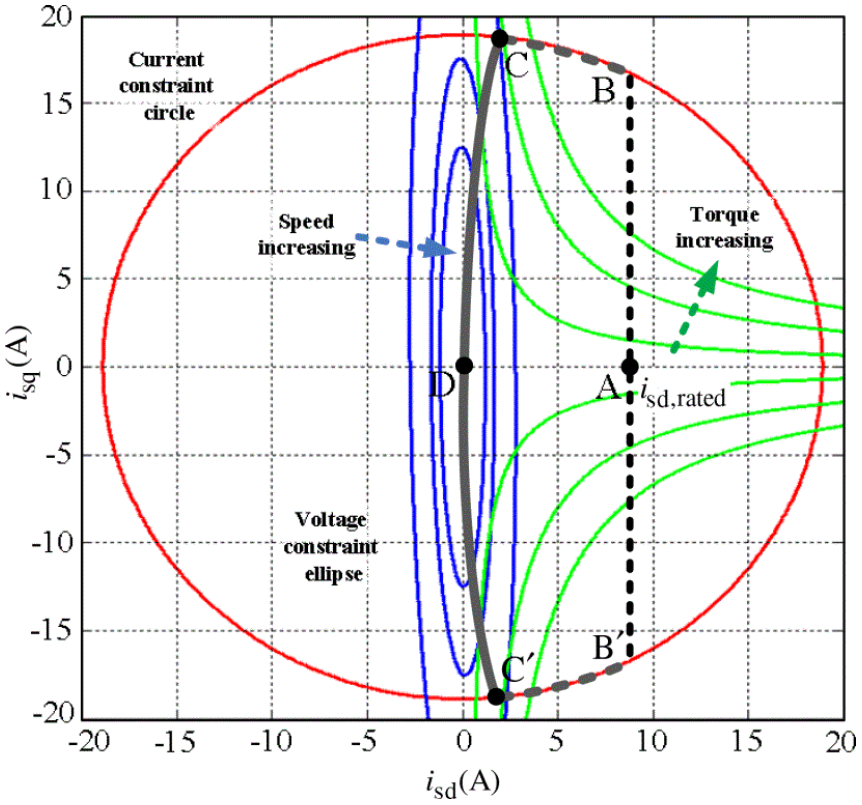


***Figure 35.*** *Field-weakening operation for induction machine in high-speed region. Modified from [22].*

### 7.3.2 Synchronous reluctance machine

Voltage equations for synchronous reluctance machine were presented in Chapter 5, which can be used to form the maximum voltage limit equation as

$$u_{s,max}^2 = \left(\omega_e L_q i_q\right)^2 + \left(\omega_e L_d i_d\right)^2 \tag{95}$$

where the stator resistance voltage drop terms have been removed to simplify the equation. This equation can be presented using current angle $\kappa$ and stator current $i_s$ with

$$u_{s,max}^2 = \omega_e^2 L_q^2 i_s^2 \cos^2 \kappa + \omega_e^2 L_d^2 i_s^2 \sin^2 \kappa \tag{96}$$

Current angle can be solved from this equation by

$$\kappa = \sin^{-1} \sqrt{\frac{u_{s,max}^2 - \omega_e^2 L_q^2 i_s^2}{\omega_e^2 i_s^2 \left(L_d^2 - L_q^2\right)}} \tag{97}$$

where the current angle has been chosen to be between the q-axis and the stator current vector.[23]

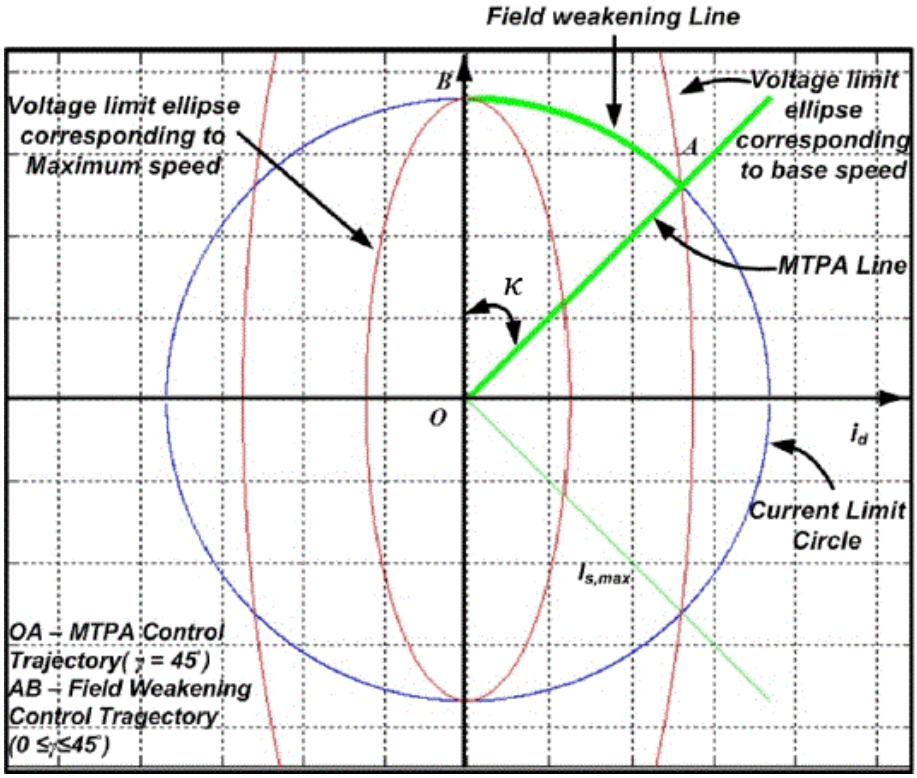


***Figure 36.*** *Field-weakening operation for synchronous reluctance machine. Modified from [23].*

Figure 36 presents the field-weakening operation for the SynRM. The Current vector is again always kept inside of the current limit circle and the voltage limit ellipse. Voltage limit ellipse shrinks as the speed is increased and the maximum torque operation point

can be found in the intersection of the voltage limit and current limit again. As speed increases when moving from point A into point B, the current angle decreases.[23]

### 7.3.3 Evaluation

When Figures 35 and 36 are compared, it can be seen, that the field-weakening line rapidly collapses for the induction machine in the high-speed region, while for the synchronous reluctance machine the operation proceeds smoothly along the current limit. This suggests that the SynRM could be capable of producing more torque in this high-speed region, since the magnitude of the current vector can be larger. Though it should be noted that the maximum torque decreases as the speed is increased. This can be observed from the SynRM torque Equation (75), where the current angle and the stator current are present. Torque receives its maximum value at 45°, and this value steadily decreases when the current angle is reduced according to sin $2\kappa$. As the speed is increased to the theoretical maximum value on the q-axis, the current angle is 0°, which produces no torque. Torque production for the induction machine can be also presented using current angle and stator current, when in Equation (84) the d- and q- currents are transformed to depend on the stator current and current angle, as was done for the synchronous reluctance machine. This would show similarly how the maximum torque drops as the speed increases until the point C in Figure 34 is reached. Since the induction machine has a higher break-down torque than the SynRM, the maximum torque for the induction machine is higher in the field-weakening region. This can change, however, in the region from point C to point D presented in Figure 35, but in this region the torque production capabilities of both of these electrical machines are minimal, as Figure 35 and torque equation for the synchronous reluctance machine suggest.

## 7.4 Energy efficiency

In Chapters 4 and 5 the structures of induction machine and synchronous reluctance machine were presented describing differences in these machines. In Chapter 6 the losses that occur in an electrical machine were presented, and according to these causes, one obvious benefit can be observed for the synchronous reluctance machine. The SynRM has no rotor windings, which completely removes copper losses associated with it. This is one of the reasons why the synchronous reluctance machine is generally more energy efficient than the induction machine[11], [20]. Synchronous reluctance machine has, however, the lower power factor, which increases the current machine takes and causes more copper losses in the stator. These results can be seen in Table 2. Also, Table 1 displays that squirrel cage induction machine has generally higher stray losses than the salient pole synchronous machine.

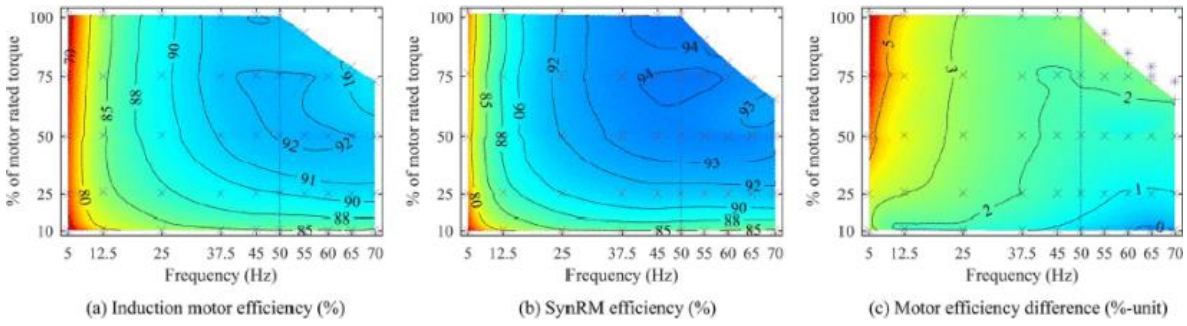


***Figure 37.*** *Comparison of SynRM and IM efficiencies with different speeds and torques. Subfigure (c) displays the efficiency increase when using SynRM compared to IM. [20]*

The efficiency difference between the induction machine and the synchronous reluctance machine also depends on the load and the speed the machine is driven at. Figure 37 presents how the efficiency difference is the greatest in low-speed and high torque region, and the lowest in high-speed and low torque area. Table 3 displays the nameplate values of these tested motors.

**Table 3.** *Nameplate values of compared IM and SynRM.[20]*

| | Induction motor | Synchronous reluctance |
|---|---|---|
| Power (kW) | 15 | 15 |
| Current (A) | 27,8 | 33,5 |
| Voltage (V) | 400 | 370 |
| Frequency (Hz) | 50 | 50 |
| Speed (rpm) | 1474 | 1500 |
| Power factor | 0,84 | 0,74 |
| Efficiency (%) | 92,7 | 94,2 |

Losses in a frequency converter can be also considered when two different motors are compared with each other. Figure 38 displays the difference in losses for IM and SynRM. It can be seen that the difference is the highest in the high torque and low-speed region, where the synchronous reluctance machine caused more losses in the frequency converter. These losses can be explained due to the lower power factor, which increases the required current[20].

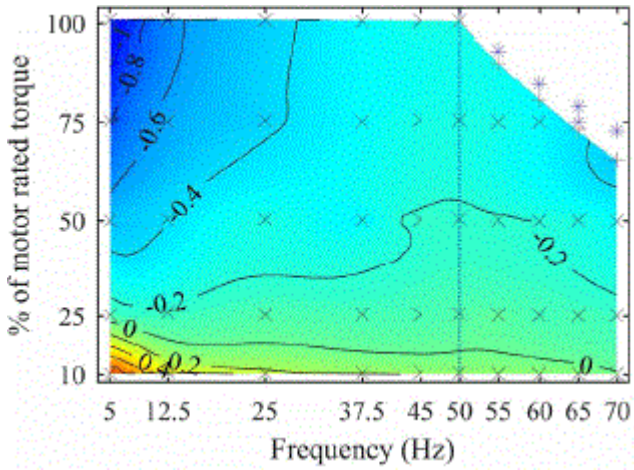


***Figure 38.*** *Difference in frequency converter losses between IM and SynRM.[20]*

## 7.5 Summary

Chapter 7.2 considered the torque production capabilities of the induction machine and the synchronous reluctance machine. It was found that the SynRM has better thermal properties, which allow the machine to produce more torque. In Chapter 7.3, the field-weakening operation was presented for the induction machine and the SynRM. This operation is mostly similar with the compared electrical machines. While nearing the maximum speed, the induction machine could produce less torque than the synchronous reluctance machine, but due to the higher break-down torque, generally induction machine produces more torque in the field-weakening region. Chapter 7.4 considered energy efficiency between the induction machine and the synchronous reluctance machine. The SynRM is more energy efficient due to the lack of rotor copper losses. The findings of this chapter are collected into Table 4.

**Table 4.** *Differences in IM and SynRM*

| | IM | SynRM |
|---|---|---|
| Torque production | Higher break-down torque. Less torque / °C | Lower break-down torque. More torque / °C |
| Field-weakening | Speed curve plummets near the maximum speed. More torque available | Smooth operation. Less torque available |
| Energy efficiency | Rotor copper losses. Slightly less stator copper losses. Lower efficiency | No rotor copper losses. Slightly more stator copper losses. Higher efficiency |

# 8. TEST SETUP AND PLANS

The theory of the synchronous reluctance machine suggests how the machine operates in different conditions, but it is important to conduct practical tests to confirm the actual behavior of the machine. This section presents details relating to the practical tests of a SynRM, other test equipment and test plans.

## 8.1 Test setup

The synchronous reluctance machine under test is tested against a load machine, which is used to generate required load torque. This setup is visualized in Figure 39. The SynRM is controlled with a certain frequency converter while the load machine has its own different control system. Frequency converter uses sensorless FOC for motor control. In this context sensorless means that the motor control does not use sensors for speed measurements. This control method follows the principles of direct FOC, which was presented in Figure 19 for the induction machine. The applied torque and mechanical speed of the motor is measured with monitoring software and sensors. Fluke Norma 4000 power analyzer is also applied to measure the active power of the motor and the active power of the whole drive system. Appendix 1 provides the configuration used for power measurements. Two test scenarios are created to inspect the behavior of the machine. In the first tests, the maximum torque of the machine is determined for different operating speeds when the output current of the frequency converter is limited to 1,5 times the nominal current of the tested motor. The SynRM can produce more torque if the machine is allowed to use more current from the frequency converter, but the limit of 1,5 times the nominal is chosen to limit the capabilities of the machine to more realistic use cases. In the second test cases the efficiency of the motor and the frequency converter is inspected when the tested motor is loaded with lighter loads, which range from 0% to 30% of the nominal torque of the motor.

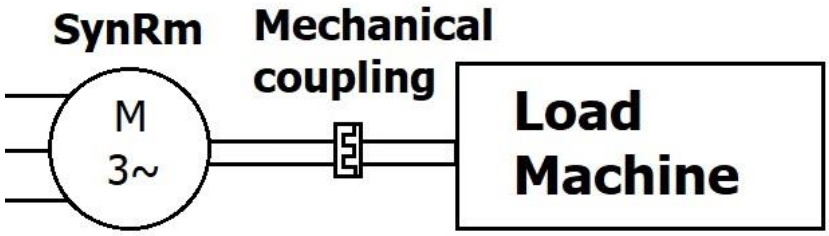


***Figure 39.*** *SynRM connected to load machine.*

## 8.2 The maximum torque test

The maximum torque for the tested motor in different speeds is determined by applying more load torque from the load machine until the motor control is unable to maintain the test speed. Recorded maximum torque in the steady state is the last torque value, where the output frequency was capable of following the frequency command at the tested speed. Tested speeds range from 0% to 170% of the nominal speed of the tested motor. Measurement points are formed by starting from 0% speed and increasing the speed in intervals of 10% of the nominal speed until the maximum speed is reached. This test is repeated three times for each measurement point. The results of each measurement point are then averaged. Each test run starts from a standstill and the motor is accelerated to the test speed. Torque is then applied from the load machine. The effects of temperature are minimized by waiting 5 minutes between each test and measuring that the hull temperature of the motor always stays below 30 °C. If the temperature rises above this limit, a longer break is taken between the measurements until the temperature is at 27 °C. The stator windings reach higher temperatures, but with this test method the difference should not be too much.

## 8.3 Efficiency test

The motor is tested with 4 different loads, which are 0%, 10%, 20% and 30% of the nominal torque. The tested speeds range from 0% of the nominal speed to 160% of the nominal. The power analyzer is used to measure the electrical input power of the motor

and the electrical input power of the whole drive. Each measurement is done as one continuous test run starting from 0% speed and the speed is increased by 10% of the nominal speed after 30 seconds have passed for different measurement points. This is done until the maximum speed is reached. Measurement data is gathered for 30 seconds per measurement point to better average the fluctuations in the input power. Each power measurement is done for the full duration of the test run. Also, each test run is performed 3 times in order to average any possible fluctuations in the test data. This is performed for 4 test loads. The temperature increase in the tested motor can be considered small with the tested loads. During these tests it is monitored that the change in temperature is always less than 6 °C from the starting temperature. The temperature is monitored in the same way as was done in the maximum torque tests. The power measurement is done first for the motor input according to the test plans that were presented above. After these measurements, measurements are done for the motor drive. It is not possible to do these measurements at the same time due to the limitations with available channels for the used power analyzer.

To solve the mechanical power of the motor, Equation (1) can be used when the output torque and the rotational speed of the shaft of the motor are known. This value is then divided by the measured input power of the motor, which forms the equation for motor efficiency as

$$\eta_{motor} = \frac{P_{mech}}{P_{motor}} \cdot 100\% \tag{98}$$

where $P_{mech}$ is the mechanical power of the motor and $P_{motor}$ is the measured electrical input power of the motor. The efficiency of the motor drive can be solved similarly by

$$\eta_{drive} = \frac{P_{mech}}{P_{drive}} \cdot 100\% \tag{99}$$

where $P_{drive}$ is the measured electrical input power of the motor drive.

# 9. TEST RESULTS AND ANALYSIS

The motor control used for the synchronous reluctance machine was also tested in various ways to make sure the motor control is adjusted properly for the tests. Frequency converter provided the motor control. The performance of the motor control was deemed satisfactory for the tests, but there was still some room left for improvements. The saliency ratio of the tested motor is 4,82, which can be considered to be somewhat low.

## 9.1 The maximum torque test

The test proceeded as planned and no major difficulties were encountered. Results of this test are displayed in Figure 40. One unexpected outcome from these tests was how the maximum torque started slowly decreasing with speeds below the nominal. This is the most prominent with the 10% speed of the nominal. It was noticed that the set current limit of the frequency converter was not reached during these speeds and the output current was somewhat lower. This finding is presented in Figure 41. The user manual of the frequency converter provided no explanation for this phenomenon. However, a guess can be formed for the reason of this behavior: the used frequency converter might limit the current that passes through it in lower speeds to protect the converter switches from reaching high temperatures that might damage them and reduce their usage time.

The maximum torque of the tested motor below nominal speed was always over 150% of the nominal. The motor can be considered usable for crane application when torque production is considered. The maximum torque values formed a straight descending line for speeds over the nominal.

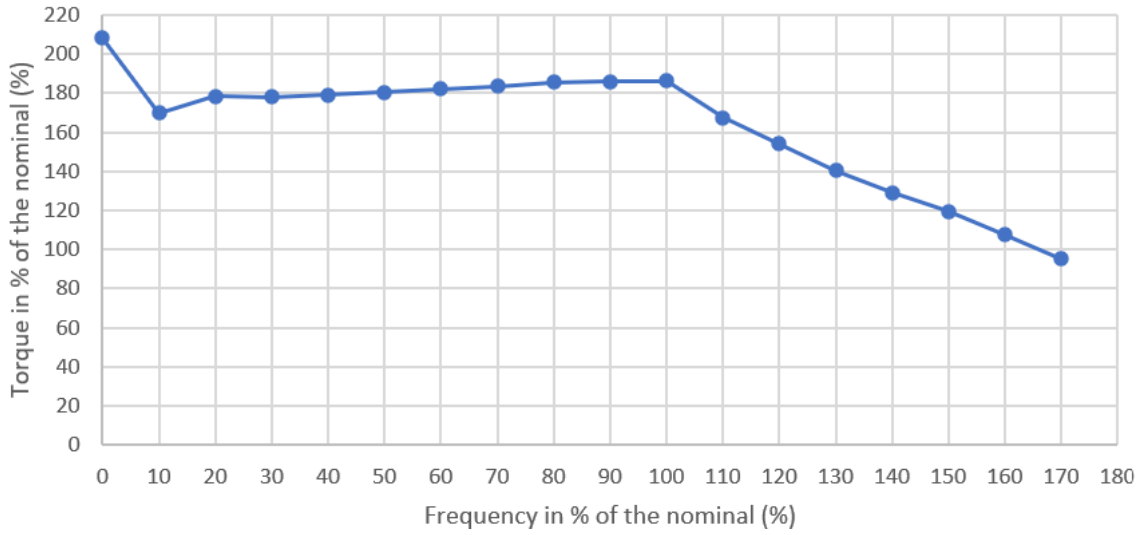


***Figure 40.*** *Maximum torque test results.*

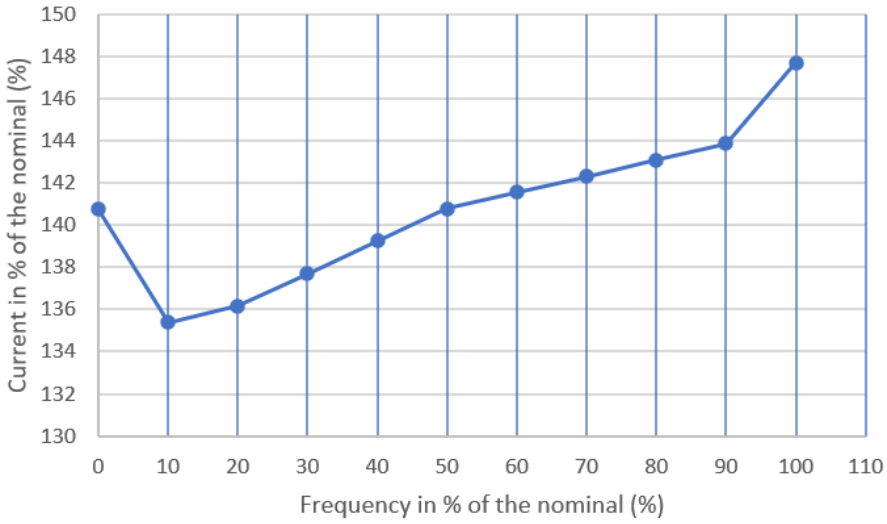


***Figure 41.*** *Decrease in output current with different frequencies.*

Other interesting result was how the motor was capable of holding a load of over twice the nominal torque in zero speed operation and how the motor control was capable of handling this. This situation responds to a possible feature for cranes called load floating, where the load is maintained stationary by producing enough torque from the motor so the load does not fall[2]. No mechanical brakes are used in this operation. Induction machines can produce problems for the sensorless motor control in zero-speed operations[24], [25], but with the tested synchronous reluctance machine the zero-speed area was controlled without problems. This result can be considered a clear advantage for the synchronous reluctance machine over the induction machine.

## 9.2 Efficiency test

Efficiency tests display that the efficiency of the test motor increases with the load, except the test cases using 20% load reached higher efficiencies than with 30% load. Efficiency results for the motor are presented in Figure 42 and results for the motor drive are displayed in Figure 43. Efficiency also increased as the speed was increased, but there was a small decrease in the efficiency of the drive in the high-speed region. Figure 37 displays that efficiency increases with load in the tested load area, which is not what the test results presented in the cases of 20% load and 30% load. During these tests a sudden instability in the output frequency was discovered in the high-speed area, which required minor changes in the parameters of the motor control. This is one possible explanation for 20% load test having higher efficiency than 30% load test. Due to this change, the test results are not accurate but can be used as indicative of the efficiency of the motor. If the test setup changes in the middle of testing, the tests should be redone. These results are used, because there was no time to redo all of them, since the thesis had a predetermined time limit. Test results can also fluctuate because the input power of the motor and the drive were fluctuating. The power analyzer records values during certain intervals, which might cause the results to differ significantly from the average. The fluctuation in the measurements was determined to be approximately ±6% of the average for the motor input and ±8,5% of the average for the drive input.  This possible error was tried to mitigate with 30 second recording time per tested speed and conducting 3 test runs for each load. However, increasing the sample size by recording each tested speed for a longer period of time and conducting more test runs than 3 would be the surest way to get results where possible fluctuations in the measured power are minimized. This was not done due to the time limitations.

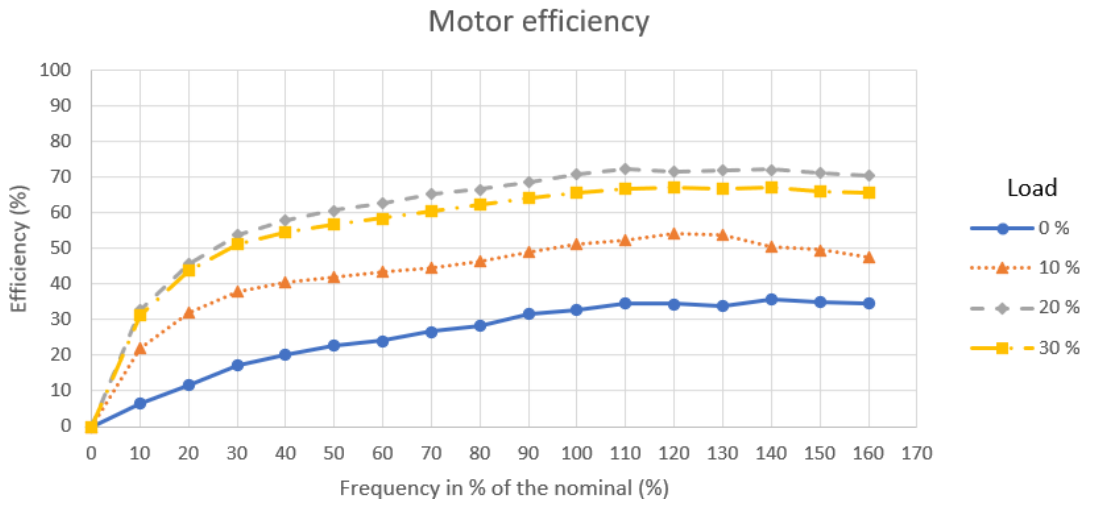


***Figure 42.*** *Motor efficiency test results.*

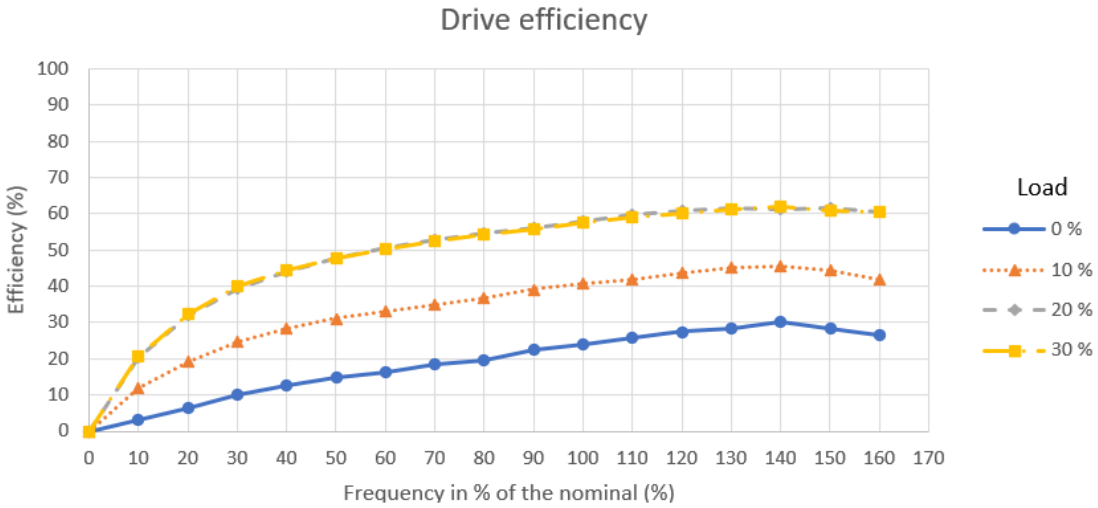


***Figure 43.*** *Motor drive efficiency test results.*

Tests showing the efficiency of the motor drive were naturally less than the efficiency of the motor, since the frequency converter losses are now also considered. This efficiency generally increased with the load, but in the cases of 20% load and 30% load tests, these efficiencies were close to each other. This result can be possible explained with the same reasons that were given to the motor efficiency measurements. However, the efficiency of the motor and the motor drive were too low to be considered for practical applications. This conclusion can be formed based on the efficiencies of other motors of the same power rating. Low efficiency can be explained with the less optimal design of the motor. The tested motor can be considered experimental. The frequency

converter is a commercial product from a certain manufacturer, which only provided limited details relating to the operation of the drive.

## 9.3 General remarks

The fastest time for acceleration and deceleration that motor control could handle was 3 seconds. These times are defined for acceleration and deceleration for the maximum speed of the motor. Better motor control and a more optimally designed motor might help with this issue. If faster speeds are required, this can cause problems for the synchronous reluctance machine. A high saliency ratio gives a faster torque response, which could help to achieve faster speeds for acceleration and deceleration. Also, Chapter 5.3.3 presents a motor control method to achieve the fastest torque response for the used motor, which could be used.

During the general testing of the motor control, the control was capable of handling sudden changes in load torque from the load machine with controlled variations in the output frequency. Figure 44 displays the results of this test. In this figure frequency command is the desired frequency and output frequency is the actual output frequency of the frequency converter. The motor was accelerated to nominal speed without any load torque and after 5 seconds nominal load was rapidly applied from the load machine, which caused a reduction in output frequency. After 10 seconds the output of the load machine was set to 0, which caused a sudden increase in output frequency. It can be seen from Figure 44 that the output frequency did not perfectly follow the frequency command during acceleration and deceleration. There was also an overshoot when the motor was accelerated from standstill to nominal speed. The motor followed speed commands accurately enough. More accurately tuned motor control could provide better results. Overall, the temperature of the test motor was relatively low during all the tests. Table 5 summarizes the results of the practical tests.

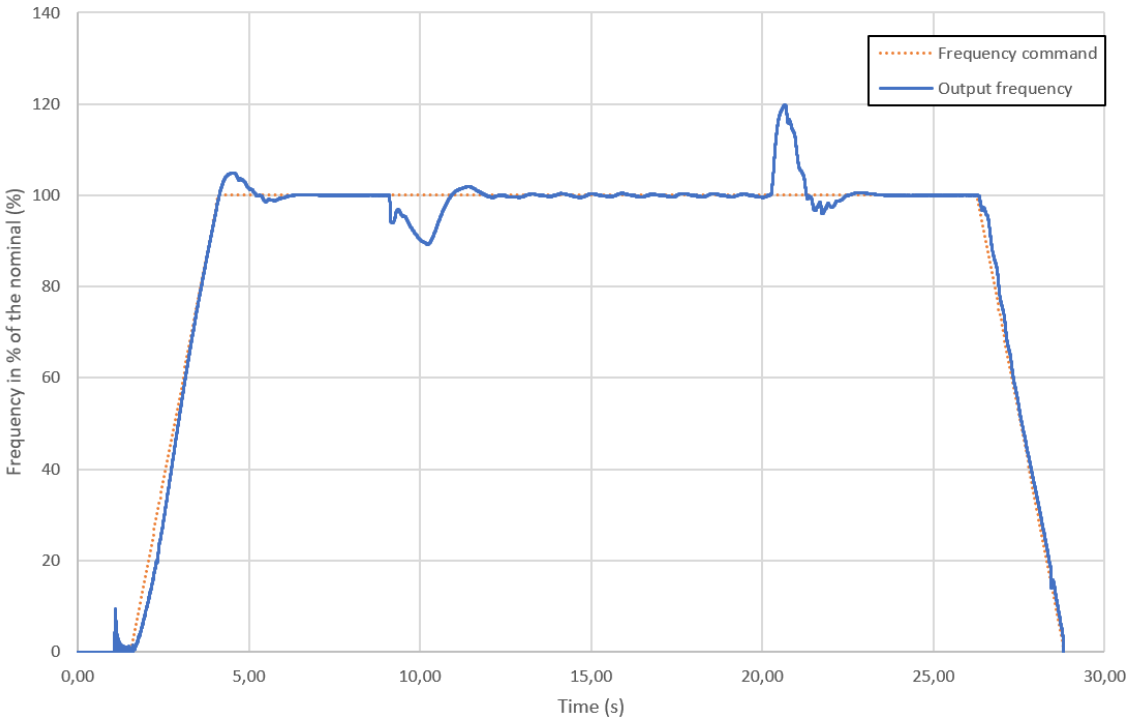


***Figure 44.*** *Fluctuations in output frequency due to sudden changes in load torque.*

**Table 5.** *Results of the SynRM drive practical tests.*

| Test | Result | Conclusion |
|---|---|---|
| Maximum torque production below nominal speed | Always well over 150 % of the nominal torque | Pass |
| Zero speed and maximum torque | Remarkable control and over 200% torque of the nominal | Pass |
| Efficiency | Highest efficiency is slightly above 60% | Fail |
| Capability to follow speed commands | Slight deviations during speed changes and small overshoots | Pass |
| Sudden load torque fluctuations | Motor control maintained stability | Pass |

# 10. CONCLUSION

The aim of this thesis was to consider the feasibility and energy efficiency of synchronous reluctance machine drive in crane application. This goal can be considered to have been partially fulfilled. Some requirements and findings were done for the SynRM, but these results can not be used to produce a conclusive declaration for the feasibility of the synchronous reluctance machine in crane applications. Useful findings were presented, which display that there is potential for this electrical machine to be used for different crane applications, but further research is required.

First, the thesis presented the basic working principles of cranes and frequency converters. Then the operational principles of induction machine and synchronous reluctance machine were presented to better compare the capabilities of the SynRM with the induction machine. The FOC motor control method was presented for both electrical machines and some variations of this control were also displayed. In the comparison of the SynRM and the IM presented in Chapter 7, it was discovered that with similarly rated machines, the SynRM has better thermal properties. For field-weakening operations it was discovered that the SynRM might operate better by producing more torque when nearing the theoretical maximum speed of the field-weakening area. Overall, the induction machine can produce more torque in the field-weakening region, as was discussed in Chapter 7.3.3. Comparative tests present that the SynRM has higher efficiency than the induction machine due to the lack of rotor windings, which removes the copper losses associated with it. The power factor of the SynRM is generally lower, which cause the machine to require more current than the induction machine, which might require a bigger frequency converter for the drive.

The synchronous reluctance machine provided for practical tests was capable of producing enough torque to be considered for crane applications. The zero-speed capabilities of the SynRM were remarkable, making the machine capable for load floating. The

efficiency of the tested motor was too low, but this was due to the experimental nature of the motor. Other provided references for motor tests present higher efficiencies for synchronous reluctance machines. The tested motor followed speed commands with enough accuracy and the motor control was capable of managing situations where there were sudden changes in the load torque. Other positive feature of the tested motor was that the temperature of the motor was always relatively low during the tests.

To conclude the findings of this thesis, the presented theory and comparative tests did not produce any arguments to forbid the use of the SynRM in crane applications. This thesis had no time to do practical comparative tests with the SynRM and the IM. For future research, this thesis suggests that feasibility for crane applications needs to be examined more closely by doing comparative tests with an induction machine, which is rated for similar use.

# REFERENCES


[1] J. Pyrhönen, V. Hrabovcová, and S. Semken, *Electrical machine drives control: an introduction*. Chichester, West Sussex, United Kingdom: Wiley, 2016.

[2] A. Halminen, Johdatus nosturitekniikkaan, Lecture slides, Konecranes, 2007.

[3] E. M. Abdel-Rahman, A. H. Nayfeh, and Z. N. Masoud, 'Dynamics and Control of Cranes: A Review', *J. Vib. Control*, vol. 9, no. 7, pp. 863–908, Jul. 2003, doi: 10.1177/1077546303009007007.

[4] J. Toivonen, 'Akkujen hyödyntäminen siltanosturin energiavarastona'. Tampere University, 2016.

[5] N. Mohan, T. M. Undeland, and W. P. Robbins, *Power electronics: converters, applications, and design*, 3rd ed. Hoboken, NJ: John Wiley & Sons, 2003.

[6] B. Drury, *The control techniques drives and controls handbook*, 2nd ed. in IET power and energy series, no. 57. Stevenage: Institution of Engineering and Technology, 2009.

[7] B. M. Wilamowski and J. D. Irwin, Eds., *Power electronics and motor drives*, 2nd ed. in The industrial electronics handbook. Boca Raton, FL: CRC Press, 2011.

[8] M. Nahalparvari, 'Fixed Switching Frequency Direct Model Predictive Control for Grid-Connected Converters', Tampere university, 2018.

[9] K. T. Chau, *Electric vehicle machines and drives: design, analysis and application*. Singapore: IEEE, Wiley, 2015.

[10] A. Emadi, Ed., *Advanced electric drive vehicles*. in Energy, power electronics, and machines. Boca Raton: CRC Press, 2015.

[11] J. Pyrhonen, T. Jokinen, and V. Hrabovcová, *Design of rotating electrical machines*, Second edition. Chichester, West Sussex, United Kingdom: Wiley, 2013.

[12] A. Omar, A. Abdulrahman, and G. Rashed, 'Direct on Line Operation of Three Phase Induction Motor using MATLAB', *J. Zankoy Sulaimani - Part A*, vol. 21, pp. 21–34, Aug. 2019, doi: 10.17656/jzs.10754.

[13] R. Moghaddam Rajabi, 'Synchronous Reluctance Machine (SynRM) in Variable Speed Drives (VSD) Applications', Dissertation, Royal Institute of Technology, Stockholm, 2011. [Online]. Available: http://kth.diva-portal.org/smash/get/diva2:417890/FULLTEXT01.pdf

[14] G. Štumberger, M. Hadžiselimović, B. Štumberger, D. Miljavec, D. Dolinar, and I. Zagradišnik, 'Comparison of capabilities of reluctance synchronous motor and induction motor', *J. Magn. Magn. Mater.*, vol. 304, no. 2, pp. e835–e837, Sep. 2006, doi: 10.1016/j.jmmm.2006.03.011.

[15] V. Burenin, J. Zarembo, O. Krievs, and L. Ribickis, 'Comparison of Synchronous Reluctance Motor and Induction Motor Efficiency Maps for Traction Application', in *2021 IEEE 62nd International Scientific Conference on Power and Electrical Engineering of Riga Technical University (RTUCON)*, Nov. 2021, pp. 1–5. doi: 10.1109/RTUCON53541.2021.9711710.

[16] A. Boglietti, A. Cavagnino, M. Pastorelli, and A. Vagati, 'Experimental comparison of induction and synchronous reluctance motors performance', in *Fourtieth IAS Annual Meeting. Conference Record of the 2005 Industry Applications Conference, 2005.*, Hong Kong, China: IEEE, 2005, pp. 474–479. doi: 10.1109/IAS.2005.1518350.

[17] A. Boglietti and M. Pastorelli, 'Induction and synchronous reluctance motors comparison', presented at the 2008 34th Annual Conference of IEEE Industrial Electronics, Orlando, FL, USA: IEEE, 13.11 2008, p. p.2041-2044. doi: 10.1109/IECON.2008.4758270.

[18] J. J. Germishuizen, F. S. Van Der Merwe, K. Van Der Westhuizen, and M. J. Kamper, 'Performance comparison of reluctance synchronous and induction traction drives for electrical multiple units', in *Conference Record of the 2000 IEEE Industry Applications Conference. Thirty-Fifth IAS Annual Meeting and World Conference on Industrial Applications of Electrical Energy (Cat. No.00CH37129)*, Rome, Italy: IEEE, 2000, pp. 316–323. doi: 10.1109/IAS.2000.881130.

[19] N. G. Ozcelik, U. E. Dogru, M. Imeryuz, and L. T. Ergene, 'Synchronous Reluctance Motor vs. Induction Motor at Low-Power Industrial Applications: Design and Comparison', *Energies*, vol. 12, no. 11, p. 2190, Jun. 2019, doi: 10.3390/en12112190.

[20] H. Karkkainen, L. Aarniovuori, M. Niemela, J. Pyrhonen, and J. Kolehmainen, 'Technology comparison of induction motor and synchronous reluctance motor', in *IECON 2017 - 43rd Annual Conference of the IEEE Industrial Electronics Society*, Beijing: IEEE, Oct. 2017, pp. 2207–2212. doi: 10.1109/IECON.2017.8216371.

[21] M. Porma, Chief development engineer, Konecranes, Interview, Jun. 29, 2023.

[22] B. Wang, Y. Zhao, Y. Yu, G. Wang, D. Xu, and Z. Dong, 'Speed-Sensorless Induction Machine Control in the Field-Weakening Region Using Discrete Speed-Adaptive Full-Order Observer', *IEEE Trans. Power Electron.*, vol. 31, no. 8, pp. 5759–5773, Aug. 2016, doi: 10.1109/TPEL.2015.2496350.

[23] S. M. Ferdous, P. Garcia, M. A. M. Oninda, and Md. A. Hoque, 'MTPA and Field Weakening Control of Synchronous Reluctance motor', in *2016 9th International Conference on Electrical and Computer Engineering (ICECE)*, Dhaka, Bangladesh: IEEE, Dec. 2016, pp. 598–601. doi: 10.1109/ICECE.2016.7853991.

[24] T. M. Wolbank and M. K. Metwally, 'Zero Speed Sensorless Control of Induction Machines Using Rotor Saliencies', in *2008 IEEE Industry Applications Society Annual Meeting*, Oct. 2008, pp. 1–6. doi: 10.1109/08IAS.2008.228.

[25] V.-M. Leppanen and J. Luomi, 'Speed-Sensorless Induction Machine Control for Zero Speed and Frequency', *IEEE Trans. Ind. Electron.*, vol. 51, no. 5, pp. 1041–1047, Oct. 2004, doi: 10.1109/TIE.2004.834965.

# APPENDIX 1: CONFIGURATION OF POWER ANALYZER

Fluke Norma 4000 power analyzer used for practical tests use the configuration presented in Table 6. The variable chosen for measuring is “Power Active” with no modifier set and phase option is set to “All Phase(1..3)”.

**Table 6.** *Timing & sync setup used for power analyzer*

| | |
|---|---|
| Averaging Intervals [s] | 0,100 |
| Sync Source | I1 |
| Sync Level | 0 % |
| Sync Slope | Positive |
| Sync Filter | 100 Hz |
| Sync Output | Off |